Chemical Processing and Micromixing in Confined Impinging Jets

Brian K. Johnson and Robert K. Prud'homme
Dept. of Chemical Engineering, Princeton University, Princeton, NJ 08544

Rapid processes such as certain organic reactions or precipitations at high supersaturation require the rapid mixing provided by jet mixers. Micromixing in a confined impinging jets (CIJ) mixer was characterized employing the Damköhler number to correlate processing. A scaling theory for the characteristic micromixing time, proportional to momentum diffusion starting at the Kolmogorov microscale, is shown as sufficient to express the micromixing performance of the CIJ mixer. A recently characterized second-order competitive reaction set is used as a "chemical ruler" to assign an absolute value to the mixing time in the CIJ mixer. A wide range of characteristic time (320 to 5 ms) is evaluated with hydrochloric acid competing for sodium hydroxide neutralization or 2,2-dimethoxypropane acid catalyzed hydrolysis. This reaction set was sensitive enough to detect the onset of a turbulent-like flow at a Re of 90 and was able to demonstrate a decrease in undesired products up to the highest Re tested, 3,800 or a jet velocity of 19 m/s. It represents a significant advancement to the reaction sets and techniques used for previous mixing studies, which are reviewed. Experiments verify the characteristic mixing time in a CIJ mixer scales as the inverse of the jet velocity to the three halves power, and the "mesomixing volume" (the volume over which the majority of flow energy was dissipated) is best approximated as proportional to the internozzle separation cubed. For each of the different jet diameters, chamber diameters and outlet configurations tested, the selectivity of the reaction scaled linearly with the Damköhler number, as determined from the known reaction kinetics and the calculated Kolmogorov diffusion time. The first full characterization is provided of micromixing in impinging jets that allows the prediction of mixing performance, reaction selectivity, and scale-up criteria.

Introduction

Our objective is to produce nanoparticles of organic compounds at high solids concentration by a "Flash NanoPrecipitation" process, which requires rapid mixing in a time less than the nucleation and growth time τ_{n+g} of a nanoparticle. The process also requires the deposition of a protective colloid on the nanoparticles at a time similar to the nucleation and growth time in order to freeze the size distribution. In this study, we present the first step to understanding the nanoparticle formation process, the rapid micromixing of two liquid streams using confined impinging jets. We wish to establish the functionality of micromixing time τ_m on the jet velocity, the stream physical properties, and the chamber geometry. This understanding has led us to develop a laboratory scale, well characterized, and simple system for probing the effects of micromixing on process performance that can be easily scaled up to production.

In the laboratory, the widely used stopped flow unit or the grid mixer (Mahajan and Kirwan, 1994) is useful for obtaining a mixing time in the millisecond range, but they can be expensive to fabricate, limited in production capacity, and prone to fouling for precipitation reactions. Impinging jets consist of two high velocity linear jets of fluid that collide to rapidly reduce the scale of segregation between the fluid streams. They have been shown to be successful at the production scale for several processes (Macosko, 1989; Demyanovich, 1991; Midler et al., 1994; Tamir, 1994). In confined impinging jets, the chamber size affects the process performance of the mixer. Unfortunately, the functional de-

Correspondence concerning this article should be addressed to B. K. Johnson at this current address: Merck & Co., Inc., P.O. Box 2000, RY818-304, Rahway, NJ 07065.

pendence of mixing time on the Reynolds number and geometry has been debated in the literature over the past 25 years leaving no clear correlation for the characteristic mixing time or scale-up criteria for confined impinging jets.

In this article we determine a simple expression, grounded in mixing theory, for the characteristic mixing time including the geometric parameters required for scale-up. A series of CIJ mixers are constructed and studied at both low and high Reynolds numbers. A recently characterized, highly sensitive and robust, homogeneous fast competitive reaction (Baldyga et al., 1998) is used to study a wider range of characteristic reaction times than those previously studied in impinging jets. This reaction is compared to two other common competitive reaction sets used for mixing characterization. A simple scaling theory is employed to understand the characteristic micromixing time in impinging jets and the relation between the Damköhler number and process performance for competitive reactions. The methodology to characterize confined mixers is also provided. Our intention is to use the confined impinging jets (CIJ) mixer as a laboratory-scale unit for the production of nanoparticles and for the rapid probing of the relation between the characteristic mixing time and process behavior for a variety of systems.

Impinging jets

We have chosen impinging jets because of their ability to deliver mixing times less than the characteristic process time for fast precipitation processes (Mahajan and Kirwan, 1996). The key to rapid mixing is twofold: (1) produce a region of high turbulent energy dissipation; (2) ensure that the process streams for mixing pass through the high intensity region without bypassing. The first criteria ensures the proper scale of mixedness and the second ensures that the desired molar flow ratios are preserved during the rapid mixing process. Bourne and coworkers have used the competitive and consecutive diazo-coupling reactions (Bourne et al., 1990, 1992a) and a mixing model to assign energy dissipation rates to process equipment under typical operation. Impinging jets rank at the top for rapid mixing and can provide energy dissipation rates up to 10^5 W/kg compared to single turbulent jets $\cong 10^4$ W/kg, rotor stator mixers $\cong 10^2$ W/kg (Demyanovich and Bourne, 1989; Bourne et al., 1992b; Bourne and Studer, 1992; Baldyga et al., 1995) and less for a stirred tank, centrifugal pump, or turbulent pipe (Bourne, 1996).

A high energy dissipation occurs for impinging jets because the kinetic energy of each jet stream is converted into a turbulent-like motion through a collision and redirection of the flow in a very small volume. Schaer and coworkers (1999) used computational fluid dynamics (CFD) to quantify the mixing volume and plot the energy dissipation rate as a function of radial position in the impingement plane for free impinging jets. The energy dissipation rate fell to 5% of the peak energy dissipation rate within seven jet diameters of the impingement stagnation point. Yeo and Wood (Yeo, 1993) examined impinging jets with CFD and concluded that most energy dissipation occurs along the jet shear layers and in the impingement plane.

Impinging jets or sheets can be considered as free, submerged, or confined. Free impinging jets collide in a large chamber where the walls have little effect on the impingement process and the chamber is filled with gas or a fluid of low enough viscosity, not to impose significant drag on the jet itself. Submerged jets are surrounded by a fluid phase of significant viscosity, enough to cause the jet to expand or entrain fluid. Confined impinging jets collide in a small chamber where the chamber size has an effect on the mixing process performance. The chamber multiple, or chamber diameter to jet diameter ratio D/d, where a free and submerged impinging jet can be considered confined, has not been elucidated, and is likely a gradual transition. In this article we examine chamber multiples of 19.0, 9.6, and 4.8 to explore the effect of chamber size on mixing.

Mixing for molecular processing

Examples of mixing-sensitive processes initiated by the combination of two fluid streams include reaction injection molding (RIM) (Kolodziej et al., 1982; Macosko, 1989), precipitation by reaction or anti-solvent addition at high supersaturation (Pohorecki and Baldyga, 1983; Garside and Tavare, 1985; Marcant and David, 1991; Mahajan and Kirwan, 1996; Baldyga and Bourne, 1999), and certain fast competitive reactions or competitive and consecutive reactions (Paul and Treybal, 1971; Baldyga and Bourne, 1990; Bourne et al., 1990, 1992a; Paul et al., 1992a; Bourne and Yu, 1994; Baldyga and Bourne, 1999). In all of these cases, the process kinetics and resulting product quality can be determined by the rate and intimacy of contacting two initially separate fluids.

To minimize the process sensitivity to mixing, one must bring the mixing characteristic time, including macromixing, mesomixing, and micromixing, below the characteristic time of the process. As shown in Figure 1, we classify the mixing of miscible fluids by three length scales: (1) "macromixing" occurs on the scale of the vessel; (2) "mesomixing" on the scale of the turbulent eddies; (3) "micromixing" on the scale of molecular diffusion in stretching fluid lamellae. In turbulent mixing, kinetic or mechanical energy input into the system is dissipated by viscous deformation during the following physical steps: (1) the distribution of fluid throughout the vessel by bulk convection (blending); (2) the formation of daughter vortices, which grow (by turbulent diffusion or inertial-convective mixing) and engulf new fluid; (3) further de-

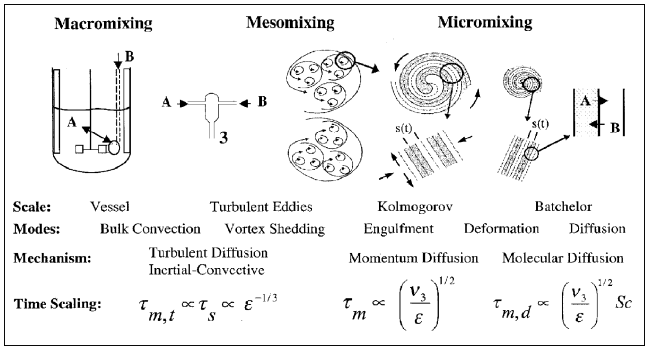

Figure 1. Fluid mixing processes following the cascade of turbulent energy from large to small scales.

A portion of the graphics for meso and micromixing are from Baldyga and Bourne (1998) and Ottino et al. (1982) reprinted with permission from John Wiley & Sons © 1999 and Cambridge University Press, respectively.

formation of daughter vortices ultimately resulting in a lamellar structure (momentum diffusion) where molecular diffusion can eliminate regions of segregation in a local flow that is laminar (molecular diffusion) (Ottino, 1982; Baldyga and Bourne, 1984, 1999; Baldyga and Pohorecki, 1995).

Molecular scale processes require micromixed fluids, and since each step in mixing is a prerequisite for the next, any of the steps can be rate limiting and control product quality. In the case of continuous impinging jets, macromixing (exchanging fluid with the bulk contents of the vessel) is not at issue since local mesomixing is all that is required to blend the two fluids. The jets collision creates a region of high energy dissipation or a mesomixing volume and all the fluid passes through this small volume. Confining the jets limits the mesomixing volume and further ensures that the two fluids are homogenized in the ratio they were charged. When comparable, the total time for homogenization of two fluid elements to a molecular level is the sum of the mixing times at each length scale. We assume here that only one mixing mechanism and associated time-scale is required to capture the range of operating conditions in this study, low viscosity fluids, and moderate velocities in a confined mixer.

Previous research on confined impinging jets

The majority of the research to characterize CIJ mixers has focused on the low Reynolds numbers characteristic of RIM, $Re = 50$ to 600. For all but the fastest processes, the mixing time of high velocity impinging jets falls below the process characteristic time and reduces the process kinetics to nearly homogeneous kinetics. Likewise, only the most sensitive measuring methods can discern the changes in process output found at higher Reynolds numbers. Typically, the experimental probes employed were not sensitive enough to capture the entire range of characteristic mixing times from the laminar well into the turbulent regime. In turn, many studies report a plateau in process performance as the Reynolds number is increased (Malguarnera and Suh, 1977; Tucker and Suh, 1978; Lee et al., 1980; Kolodziej et al., 1982; Baldyga and Bourne, 1983; Sandell et al., 1985). In contrast, Nguyen and Suh (1985) found no such plateau as the Reynolds number was increased. Due to the conflicting conclusions, a clear picture of the effect of a characteristic micromixing time on process performance cannot be stated. The previous research to characterize the confined impinging jets is reviewed in this section to provide additional motivation for more studies on impinging jets, and to demonstrate some advantages of the reaction system chosen in this article for measuring process performance.

Low Reynolds Number Experimental Probes. Malguaranera and Suh (1977) found a reduction of the standard deviation in the titration of small random samples from the mixing of glycerin, with and without an acid component, up to a Reynolds number of 500. They found no further change up to a *Re* of 3,000 since the standard deviation in the measurement was greater than that caused by the mixing process. Likewise, Tucker and Suh (1978) looked at the standard deviation in light transmitted from the mixer output created by mixed clear and dyed streams using a sample volume of characteristic length one-half the jet diameter. They found stratified fluids below a *Re* of 80, turbulent results from *Re* of 150 up to 600, and undetectable differences beyond that value. Lee et al. (1980) found an increase in the adiabatic temperature rise of polyol and isocyanate polymerization up to a critical Reynolds number after which no improvement was detected. As the reaction gel time decreased from 49 to 6 s the Reynolds number increased from 80 to 240 in order to achieve the maximum adiabatic temperature rise in the system. This was a clear sign that the characteristic mixing time fell below the reaction time near the critical Reynolds number and a maximum conversion was reached. In contrast Kusch et al. (1989) determined that an increase in the Reynolds number was not required to reach the same reaction selectivity, as the characteristic reaction time was decreased by a factor of four (Figures 3 and 9 in their article). They employed a sensitive fast competitive and consecutive diazo coupling of Bourne (Bourne et al., 1990) as in Eq. 5 below, but chose their characteristic reaction time to be similar to a RIM gel time (3–12 s), well below the capacity of turbulent jets to mix the reagent streams. By a Reynolds number of 500, the variation in the reported selectivity was comparable to the absolute value since the characteristic reaction time was surpassed. Unexpectedly, the selectivity was found to plateau at different values due to the incomplete conversion of the limiting reagent, a difficulty of this reaction system. Kolodziej et al. (1982) measured the mixing quality by optical microscopy of the striation thickness distribution of a urethane polymerization with one stream containing carbon black. They measured the same striation thickness distribution for a *Re* of 250 and 450. Their data was explained by Baldyga and Bourne (1983), emphasizing there is no effect of Reynolds number on striation thickness distribution in the inertial-convective subrange. Sandell et al. (1985) monitored the oscillation frequency of fading dye in the impingement plane to determine a significantly enhanced mixing quality up to a *Re* of 250, followed by a slow improvement up to the highest *Re* tested, 720. Visual observations and photographs of the same system showed a significant enhancement of mixing quality up to a *Re* of 400.

All of these studies were performed in confined impinging jets with a D/d of 2 to 5. They showed a plateau in process performance where the process measurement did not continue to rapidly improve. In most cases, the conclusions drawn at high *Re* were constrained by limitations in the assays used to quantify the level of mixing.

Higher Reynolds Number Experimental Probes. We have only found one experimental study correlating the process output of confined impinging jets which was sensitive enough to study low and high Reynolds numbers above $Re = 600$. Nguyen and Suh (1985) examined the impingement of three streams, two reactive and one inert. By extracting the inert monomer from the polymerization of polyol and isocynate, they could measure the domain size of the inert compound and relate this to the mixing performance. They did not see a plateau in process performance over the range of Reynolds numbers tested, 300 to 4,000. Unfortunately, their results are convoluted by interfacial tension and coalescence of the inert stream after impingement and prior to polymer network formation. Indeed, the inert domains they measured were round and large, $> 10\ \mu$m. Therefore, we are hesitant to extrapolate their findings to other processes or to a correlation of characteristic mixing time.

Mahajan and Kirwan (1996) were close to investigating the micromixing and process performance in confined impinging jets, but they studied a larger range of chamber multiples,

$D/d = 12$ to 50 in a single mixing chamber with the jets spacing kept constant. They probed the Reynolds numbers up to 2,500 by extending the common diazo-coupling reaction to a characteristic reaction time of 65 ms by increasing the reaction temperature and running near the limit of reagent solubility. Similar to Kusch et al. (1989), they also reached the point where the micromixing exceeded the sensitivity of the reaction measurement as the Reynolds number was increased. Like Demyanovich and Bourne (1989) for free impinging sheets, Mahajan and Kirwan assumed that the jets were free from the effects of the chamber walls and used a scaling model of molecular diffusion starting at the Kolmogorov length scale as the active mechanism to correlate the micromixing time. In this article, we study highly confined impinging jets and push the characteristic mixing times an order of magnitude lower to 5 ms, a time-scale sufficient for the production of nanoparticles. In addition, we demonstrate momentum diffusion to be the active mechanism of micromixing in a CIJ mixer.

Computer Enabled Research. With the advancement of readily available computing power, studies using particle image velocimetry (PIV), laser induced fluorescence (LIF), laser doppler anemometry (LDA), or (CFD) have provided insight into the flow patterns of confined impinging jets, but do not directly link their findings to processing output or are limited to lower Reynolds numbers (Wood et al., 1991; Johnson et al., 1996; Unger et al., 1998; Zhao and Brodkey, 1998; Unger and Muzzio, 1999; Johnson and Wood, 2000). Baldyga and coworkers (Baldyga, 1994; Baldyga and Henczka, 1995; Baldyga and Orciuch, 1997) have reviewed turbulence closure models and accurately modeled turbulent processing in confined mixers, but the approach requires *a priori* knowledge of the state of mixedness, an energy dissipation map of the reactor. In general, the closure methods for CFD of turbulent processing must be verified using complementary experimental results. Until these simulations become validated and routine, there is a strong need for further understanding of the process performance. The accurate and sensitive experimental studies in this article provide additional data for comparison to simulations.

Research Method

Absolute mixing time

The process performance in a mixer can be separated into dimensionless groups countributing to the "homogeneous" kinetics of the process, such as the ratio of molar charges of reagents and kinetic constants, and groups "transport controlled" in nature. When the variables contributing to homogeneous kinetics are held constant, the transport controlled effects can be contained within the Damköhler number for the process. In this article, sets of competitive reactions are conducted in the CIJ mixer. The fraction of undesired product formed X is measured as a process output and is considered to be a unique function of the Damköhler number, or the ratio of characteristic times for mixing and reaction

$$X = f(Da) = f\left(\frac{\tau_m}{\tau_r}\right) \tag{1}$$

With knowledge of τ_r and X, information on τ_m can be determined. Thus, our approach to understanding processing in the CIJ mixer is as follows:

(1) Assume each value of Da produces one value of X.

(2) Measure X after mixing for many reaction time constants (that is, reagent concentrations), jet Reynolds numbers (velocity), viscosity, and mixer geometry.

(3) Calculate τ_r from known reaction kinetics and reagent concentrations by Eq. 3 below.

(4) Employ a scaling theory to link the jet velocity, viscosity, and mixer geometry to the resulting mixing length scale and associated characteristic mixing time as

$$\tau_m = K_{CIJ} \cdot \text{scaling relationship}$$

(5) Superimpose the data (X vs. $Da = \tau_m/\tau_r$) for all conditions to determine parameters in the scaling relationship.

Knowledge of the prefactor K_{CIJ}, or any prefactors for the relation between X and Da, is not required to obtain the scaling relationship. Provided that the mixing mechanism does not change in the range of evaluation, we expect to see a single "master curve" that contains all the data collected. This is our signal that we have properly scaled the characteristic mixing time. As part of this exercise, we will obtain the functional form of Eq. 1 for parallel reactions. Therefore, the work can be extended to other reactions of the same type.

We wish to determine an expression for the absolute mixing time in the CIJ mixer and, at the same time, determine the absolute relation between X and Da for future reference. If the scaling relationship for the mixing time is known for a set of conditions (via steps 1 to 5), a single measure of the mixing time by an independent method will provide the prefactor K_{CIJ} in step 4. Thus, a final step is used to develop an analytical CIJ mixer:

(6) We alter the geometry of the mixer and record the point where the exit configuration no longer effects the reaction conversion X. We define the absolute mixing time as equal to the residence time for this condition.

This assignment of an absolute mixing time is enabled by a proper choice of the test reaction system coupled with two salient observations. First, the acid-base fast competitive reaction is several orders of magnitude faster than the mixing process. Thus, the fluid mixing is rate limiting and the time for neutralization matches the mixing time. Second, the conversion for the slow competitive reaction can change only if the neutralization reaction (or mixing) is incomplete. Thus, observing the effect of the outlet configuration for a mixer can be used to identify whether the mixing process is completed within the residence time of the mixer.

For future reference, the competitive reaction set is characterized:

(7) Quantify the prefactor(s) for Eq. 1 by measurement of the fraction of conversion and calculation of $Da = \tau_m/\tau_r$ for a variety of conditions.

A dividend of the work to quantify the absolute mixing time for the CIJ mixer is the definition of a standard reaction set where the absolute relation between fraction conversion and Damköhler number is known. Thus, other confined mixers can be characterized for absolute mixing time using only steps 1 to 5 or a subset. For the reactions in this article, it is demonstrated X and Da are directly proportional over the

range of interest and $Da = 1$ at $X = 0.04$ ($X = 0.04\ Da$). Thus, $X = 0.04$ is used as a physical reference point within figures throughout the article.

In order for the above methodology to work, we must choose a well characterized test system that is sensitive in the range of interest and we must propose a mixing scaling model to express the characteristic mixing time.

Competitive reactions

We take advantage of the sensitivity and flexibility of chemical reactions to determine an expression for the characteristic mixing time obtained by a CIJ mixer. Reactions with well defined kinetics are used as "chemical rulers" to characterize the striation length scales and micromixing time. Second-order competitive reactions are employed

$$A + B \xrightarrow{k_1} \text{Products} \qquad \text{Fast} \tag{2a}$$

$$D + B \xrightarrow{k_2} \text{Products} \qquad \text{Slow} \tag{2b}$$

The fast reaction is the neutralization of acid and base, which is essentially instantaneous relative to the mixing. The slow reaction is the hydrolysis of reagent D, either dimethoxypropane (DMP) (Baldyga et al., 1998) or ethylchloroacetate (Bourne and Yu, 1994). Reagent B (acid for the DMP and base for the ethylchloroacetate) is mixed with a stream of A and D with all molar ratios near one. In the case of DMP hydrolysis, the reaction is catalytic and reagent B is also a product. A simple illustration of why these reactions are mixing sensitive is given in Figure 2 by two cases: (a) When the characteristic mixing time τ_m is small relative to the characteristic reaction time of the slow reaction τ_r, the reaction kinetics approach the homogeneous condition, and, since $k_1 \gg k_2$, the fractional yield of the slow reaction X is not detectable; (b) When the mixing time of reactants is comparable to the characteristic reaction time, a segregated lamellar structure or unequal molar ratios exists locally during the reaction. In the interfacial region, reagent A will immediately react with B leaving reagent A depleted locally relative to D. Reagent D continues to diffuse toward B and has the opportunity to react, resulting in a detectable fractional conversion.

Since the reaction rate constants in Eq. 2 are different by many orders of magnitude and the fast reaction is essentially instantaneous relative to the mixing, the characteristic reaction time τ_r can be expressed as the pseudo first-order time constant of the slow reaction (Baldyga and Pohorecki, 1995)

$$\tau_r = 1/k_2 C_{Bo} \tag{3}$$

In Eq. 3, the initial concentration of reagent B, C_{B0}, is the average concentration after mixing as if no reaction had occurred. This applies at all flow ratios F.

The measure of process output X is defined as the fraction of D reacted

$$X = 1 - \frac{N_D}{N_{Do}} \tag{4}$$

N_{Do} and N_D are the molar flow rate of species D in moles per second before and after the reaction, respectively. The use of conversion is convenient because it reflects the segregation history of all the fluid elements (an average result) and can be measured off-line, after the reaction is completed. For a reaction that is not catalytic and with molar ratios all of one, X has the same value as the commonly used variable X_Q or the fraction of the limiting reagent B used to produce Q.

Two previous studies on impinging jets (Kusch et al., 1989; Mahajan and Kirwan, 1996) have employed the competitive and consecutive coupling of diazotised sulfanilic acid (B) with 1-naphthol (A) to form mono-azo dye (R), competing with a further reaction of R with B to form bis-azo (S) (Bourne et al., 1990). These reactions follow the form of Eq. 5 with the selectivity X_s, defined as the fraction of limiting reagent B used to produce reagent S

$$\mathrm{A} + \mathrm{B} \xrightarrow{k_1} \mathrm{R} \qquad \text{Fast} \tag{5a}$$

$$\mathrm{R} + \mathrm{B} \xrightarrow{k_2} \mathrm{S} \qquad \text{Slow} \tag{5b}$$

$$X_S = \frac{2C_S}{2C_S + C_R} \tag{6}$$

We have avoided this set of reactions, because it is too slow for the rapid micromixing studies in the CIJ mixer, those required to match the time-scale of nanoparticle formation. We did not use the "improved" Bourne reaction including 2-naphthol with A in Eq. 5 (Bourne et al., 1992), which is sensitive enough for impinging jets, because the reagents lack stability and the analysis requires multiple component regression of UV spectra vs. the simple and sensitive gas chromatography (GC) analysis employed in this article.

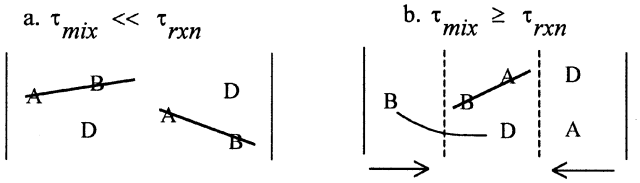

Figure 2. Depiction of micromixing effects on the product distribution of second-order competitive reactions.

(a) Mixing rapid enough to achieve homogeneous kinetics and undetectable conversion of the slow reaction. (b) Mixing resulting in striations of reagent streams, reaction (likely at incorrect volume ratios), and detectable conversion of the slow reaction.

Micromixing scaling theory

Characteristic Mixing Time. We adopt a scaling model for the characteristic mixing time, which is equal to the diffusion across a length scale characteristic of the mixing energy input into the system. The time for diffusion can be approximated using half the slab thickness, due to a repeating boundary condition

$$\tau_m = \tau_{\text{diffusion}} = \frac{(0.5\lambda_K)^2}{\text{diffusivity}} \tag{7}$$

The length scale for the slab is chosen to be the Kolmogorov length scale λ_K or the smallest eddy dimension which is able

to form in turbulence prior to the domination of viscous effects and a laminar flow microstructure. The diffusivity can be chosen as that for molecules (Mahajan and Kirwan, 1996; Demyanovich and Bourne, 1989) or momentum. We have shown (as will be shown in Figure 8) the momentum diffusivity or the kinematic viscosity ν in m^2/s to be appropriate for the CIJ mixer. We assume here that mixing down to the Kolmogorov scale is not rate limiting and a "lamellar" structure can be created fast relative to the diffusion time of the reagents in the system. The length scale can be expressed in terms of the energy dissipation rate ϵ in $J/s \cdot kg$, and the kinematic viscosity existing at the point of mixing

$$\lambda_K = \left[\frac{\nu_3^3}{\epsilon} \right]^{1/4} \tag{8}$$

Demyanovich and Bourne (1989) have demonstrated the best choice for the viscosity is that of the effluent, or stream 3. The energy dissipation rate is simply the rate of energy input into the system P in J/s, divided by the mass over which the energy is dissipated, expressed as the product of the mesomixing volume V_m in m^3, and the density ρ in kg/m^3

$$\epsilon = \frac{P}{\rho_3 V_m} \tag{9}$$

Giving

$$\tau_m \propto \frac{1}{4} \left(\frac{\nu_3}{\epsilon} \right)^{1/2} \propto \frac{\nu_3^{1/2} \rho_3^{1/2} V_m^{1/2}}{4P^{1/2}} \tag{10}$$

We assume here the energy is dissipated during mixing in a homogeneous fashion and a single Kolmogorov length scale characterizes all striations leaving the mesomixing volume. Choosing an average length scale may not be unreasonable since Kusch et al. (1989) have shown little change in process predictions vs. the distributed length scales, known to exist under conditions of homogeneous reaction and high mixing intensity (Kolodziej et al., 1982; Baldyga and Bourne, 1983). This model also does not explicitly include lamellae stretching of the fluid slabs after formation (Ottino, 1982; Kusch et al., 1989), but it is inherent in the momentum diffusion mechanism.

The energy input to the system can be derived from the redirection of each stream's velocity into the perpendicular direction. The rate of kinetic energy input into the system can be expressed in terms of the mass-flow rate m in kg/s and the velocity of the incoming streams u_y in m/s

$$P \propto \left(\frac{1}{2} m_1 u_{y1}^2 + \frac{1}{2} m_2 u_{y2}^2 \right) \tag{11}$$

Equation 11 states that the y-component of kinetic energy characterizes the energy used for turbulent mixing. In the extreme, the collision is inelastic, as assumed by Mahajan and Kirwan (1996) for free impinging jets with an impingement angle of 154° and shown to be accurate by Demyanovich and Bourne (1998) for free impinging sheets with an impingement angle less than 120°. For jets impinging at a 180° angle, we expect the collision to be somewhat elastic, since energy is required to accelerate the fluid in the perpendicular direction. We assume a proportionality constant would be sufficient to account for the elastic behavior. We later show the velocity of fluid exiting a mixer with a large size chamber is not relevant to the process performance, it only increases the pressure drop across the mixer. Thus, we draw our control volume prior to the exit constriction. Since the chamber diameter is at least 4.8 times the jet diameter, we have not considered the kinetic energy of the exit stream explicitly. Alternatively, in cases where the exit velocity cannot be ignored, one can simply assume that the energy dissipation is proportional to a representative velocity cubed ($\propto mu^2 \propto u^3$) and determine the dependence on flow ratio and geometry experimentally (Johnson, 2003).

In order to correspond with findings for free impinging jets, we match the momentum of each jet to create a stable impingement plane

$$m_1 u_{y1} = m_2 u_{y2} \tag{12}$$

or

$$\frac{d_1}{d_2} = \frac{Q_{F,1}}{Q_{F,2}} \left(\frac{\rho_1}{\rho_2} \right)^{0.5} \tag{13}$$

We can combine the previous to yield the rate of energy input

$$P \propto \frac{\pi}{8} d_1^2 u_1^3 \rho_1 \left(1 + \frac{m_1}{m_2} \right) \tag{14}$$

A combination with Eq. 10 leads to the characteristic micromixing time of impinging jets

$$\tau_m \propto \frac{1}{\sqrt{2\pi}} \frac{\nu_3^{1/2} V_m^{1/2}}{d_1 u_1^{3/2} \left(\frac{\rho_1}{\rho_3} \right)^{1/2} \left(1 + \frac{m_1}{m_2} \right)^{1/2}} \tag{15}$$

The characteristic mixing time relies on the construction of a mesomixing volume V_m of unknown geometric dependence and size. We consider the mesomixing volume to be that over which the majority of the energy used for turbulence is dissipated. CFD simulations could be useful to define this volume as, for example, the size where 90% of the turbulent energy is dissipated. For this article, the key physical dimensions we change are those of the jet diameter $d_1 = d_2$ and internozzle separation I expressed as the chamber multiple $\Delta = I/d_I = D/d_1$. The length of the mixing chamber has been restricted to twice the internozzle separation or twice the diameter. On dimensional grounds, the mesomixing volume can be expressed as a simple power function of these two lengths

$$V_m \propto I^y d_1^x = \Delta^y d_1^{y+x} \qquad y + x = 3 \tag{16}$$

The volume V_R of our CIJ mixer with a conical outlet is exactly the volume of a cylinder with a height twice the diameter

$$V_R = \frac{\pi}{2} (I)^3 = \frac{\pi}{2} \Delta^3 d_1^3 \tag{17}$$

As a physical reference, we choose the coefficient of Eq. 16 as $\pi/2$.

In the current study, the viscosity of stream one, defined as containing acid, and the effluent stream were within 5%. Likewise, the density of all streams were within 1% equal mass-flow rates were used for each reagent stream, and the jets were of equal diameter. Finally, accounting for these contributions and combining Eqs. 15 and 16, the characteristic mixing time is

$$\tau_m \propto \frac{1}{2\sqrt{2}} \frac{\nu_3^{1/2} \Delta^{y/2} d^{1/2}}{u^{3/2}} \tag{18}$$

The development of Eqs. 15 and 18 has been simplified by assuming the Kolmogorov microscale is attained fast relative to molecular diffusion, molecular diffusion is not important for the mixing time, a single length scale can adequately characterize the striation distribution formed in the mixer, and the y-component of kinetic energy is proportional to the power used for turbulent mixing in the reactor.

Damköhler Number. Combining Eqs. 3 and 18 yields the dimensionless Damköhler number

$$Da = \frac{\tau_m}{\tau_r} \propto \frac{1}{2\sqrt{2}} \frac{\nu^{1/2} \Delta^{y/2} d^{1/2}}{u^{3/2}} k_2 C_{Bo} \tag{19}$$

Our objective is to verify the functional form of Eq. 18, including the mixing mechanism and relation prefactor, through experiments. From the process scaling theory, the dependence of the Damköhler number on velocity, kinematic viscosity, and jet diameter is determined. Only the dependence of characteristic micromixing time on internozzle separation and the relation prefactor is unknown. Again, we assume an equal fractional conversion corresponds to an equal Damköhler number. In other words, the expression in Eq. 1 is single valued. The proper scaling law has been determined when the individual curves of X vs. Da for each process condition or geometry overlap.

Experimental Studies

Apparatus

Figure 3 displays the apparatus used for the impinging jets. A positive displacement constant fluid flow was provided by two microprocessor controlled syringe pumps (Harvard Apparatus, model 70-2023). Glass, gas tight syringes (SGE Inc.) of 100 cm^3 each were calibrated and used for fluid delivery. A total of four syringes could be loaded on each pump, and the majority of runs were completed using both reagent streams supplied by a single syringe pump. The pressure of each stream was measured by a small displacement diaphragm pressure transducer (Celesco, model PD7) connected to an analog paper chart recorder (Yokogawa, model 3021). The maximum pressure was limited by two 75 psig pressure relief valves for safe operation with glass syringes. This pressure limited the maximum flow rate attainable for the mixing units with jet diameters of 250 and 500 μm. All tubing leading to the jet mixer was 1/16 in. I.D. Teflon tubing. Each data point could be collected using less than 20 cm^3 of solution. All temperature measurements were made using a calibrated hand held microprocessor thermometer (Omega, model HH23).

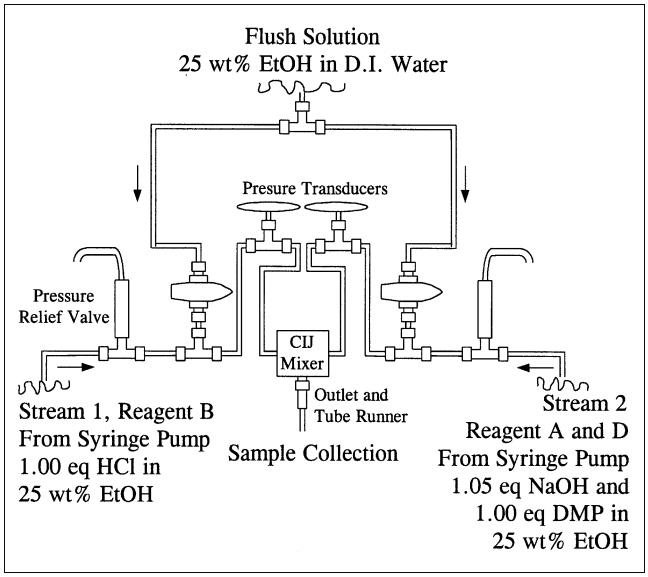

Figure 3. CIJ Mixer apparatus for the competitive reactions of neutralization and dimethoxypropane acid hydrolysis.

CIJ mixer design

Several mixing heads with different outlets were evaluated, as depicted in Figure 4 and Table 1. The impingement heads were constructed of Delrin. The collinear alignment of the impinging jets was ensured by microdrilling a single hole to create both jets. The jet diameter to run ratio L/d was a minimum of 8 to ensure the jets were stable (Mahajan and Kirwan, 1996). The chamber height to diameter ratio $H = 0.8D$, and length to diameter ratio $H + Z = 2.0\ D$ were held constant to maintain geometric similarity upon scale-up. The exit tube runner was at least ten times the outlet diameter $K/\delta = 10$, in order to ensure the streams were fully reacted prior to sample collection. The outlets of the mixing chamber were either conical, square, or a helical static mixer designated by Y, S and M, respectively. The diameter of the outlet hole δ was designated as a multiple of the jet diameter. Figure 4 and Table 1 provide the notation and dimensions for each mixing head evaluated. For example, unit 500A-Y2X corresponds to a jet diameter of $d = 500$ μm, a series A unit or $D = 4.76d$, and an outlet fitting of the conical type with an outlet hole equal to two times the jet diameter or $\delta = 1{,}000$ μm.

Competitive reaction systems

Baldyga et al. (1998) developed a competitive reaction scheme which is fast enough for impinging jets, has stable reactants and products, and is easily quantified by gas chromatography. The fast reaction is the neutralization of sodium hydroxide with a second-order rate constant $k_1 = 1.4 \times 10^8$ $m^3/mol \cdot s$ and exothermic heat of reaction $\Delta h_1 = 55.8$ kJ/mol

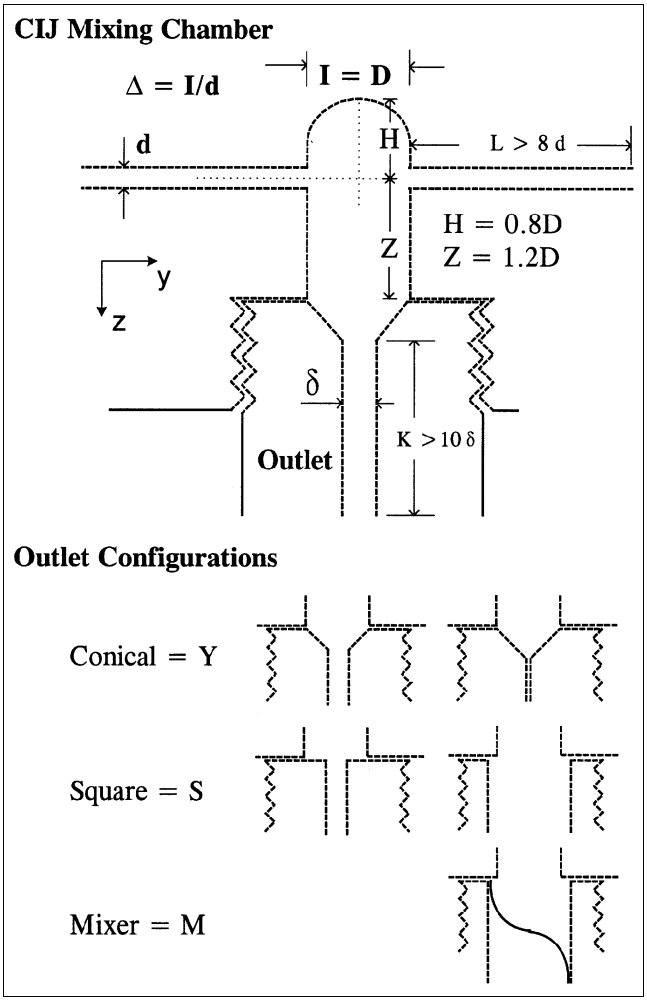

Figure 4. CIJ Mixer notation.

at 298 K

$$OH- + H^+ \rightarrow H_2O \quad (20)$$

$$CH_3C(OCH_3)_2CH_3 + H^+ (+H_2O) \rightarrow CH_3COCH_3 + 2CH_3OH + H^+ \quad (21)$$

The slower reaction is the acid catalyzed hydrolysis of 2,2-dimethoxypropane (DMP) to form one mole of acetone and two moles of methanol. The reaction is slightly endothermic, $\Delta h_2 = 18.0$ kJ/mol. In order to enhance the solubility of DMP in water, the solutes are dissolved in a solvent that is 25 wt. % ethanol. The ubiquity of water in the system allows the hydrolysis rate expression to be simplified to second order with a second-order rate constant for the hydrolysis as shown in Eqs. 22 and 23. When water is excluded from the previous reaction set, the system reduces to that of simple parallel reactions, Eq. 2 where B is catalytic acid and D is the concentration of DMP.

$$r = \frac{dC_{DMP}}{dt} = k_{H+} C_{DMP} C_{H+} \quad (22)$$

where

$$k_{H+}\,(\mathrm{m^3/mol \cdot s}) = 7.32 \times 10^7 \exp(-5556/T)\, 10^{(0.05434 + 7.07 \times 10^{-5} C_s)} \quad (23)$$

The rate constant was obtained by Walker for sodium chloride concentrations C_s of 100 to 1,200 mol/m^3 and a temperature range of 298 to 313 K. The rate expression and rate constant was determined using a stopped flow apparatus with a 1:1 stream and molar ratio, similar to our experimental studies, and was verified over the range of 25 to 1,333 moles HCl/m^3. The heat capacity of the solutions pre and post mixing was 4.2 kJ/kg·K from 296 to 306 K.

We have measured the viscosity and density of our reaction solutions and effluent and found they can be accurately fit by

$$\rho_{1,2,\text{or }3}(\mathrm{kg/m^3}) = 1143.9 - 0.60916T + 0.020894C_{\text{init}} + 0.014989C_{\text{NaOH}} \quad (24)$$

$$\eta_{1,2,\text{or }3}(\mathrm{mPa \cdot s}) = 36{,}780 \exp(-0.03296T) + 1.20 \times 10^{-4}(1 - X)C_{\text{init}} + 7.00 \times 10^{-4} C_{\text{NaOH}} \quad (25)$$

Here, C_{init} is the initial concentration of DMP or HCl before mixing, C_{NaOH} is the concentration in the stream of interest (both in mol/m^3), T ranged from 294 to 311 K, and X is the fraction of DMP converted. Note that the absolute solvent content varied from 25 to 22.7 wt. % ethanol as the starting concentration of solutes increased over the range evaluated, 8.6 to 600 mmol/L DMP, respectively. This change is inherent in the viscosity and density fit. The viscosity was measured using an automated Ubeholde viscometer (Schott, model CT460 and AVS 360 with a 53110 Type I capillary). The viscosity of the DMP and NaOH starting solution was at most 25% higher than the stream containing HCl and the reaction effluent, both lacking significant NaOH and near a viscosity of 2 mPa·s. We have also investigated the stability of the DMP starting reaction solution. Based on the GC response of either DMP or MeOH, the decomposition rate was less than 0.6% per day for 30 days at room temperature and 200 mmol/L DMP.

A second competitive reaction with the form of Eq. 2, the base hydrolysis of ethylchloroacetate, was also investigated

$$HCl + NaOH \rightarrow NaCl + H_2O \quad (26)$$

$$CH_2ClCOOC_2H_5 + NaOH \rightarrow CH_2ClCOONa + C_2H_5OH \quad (27)$$

The details of this reaction system were presented by Bourne and Yu (1994). The second-order rate constant for the slower reaction was $k_2\ (\mathrm{m^3/mol \cdot s}) = 2.0 \times 10^5 \exp(-4680/T)$, where T is in K. We found this reaction less versatile than the DMP reaction, because the minimum characteristic reaction time is limited by the ethylchloroacetate solubility and the decomposition of ethylchloroacetate can be acid catalyzed prior to jet mixing the two streams. Ethylchloroacetate in the starting reaction solution at 130 m^3/mol degraded 4.5% in 30 min at 32.5°C. Thus, reaction solutions were used immediately after adding ethylchloroacetate and reaction effluent samples were immediately diluted with water to slow the

reaction and frozen on dry ice until G.C. analysis for ethanol. The physical properties of water were used for data analysis. The experimental protocol used for this reaction matches that of the DMP hydrolysis described below.

Run protocol

The molar ratio of reagents for all runs was kept at 1.05:1.00:1:1.00 ± 0.01 for A:B:D, as listed in Eq. 2. Each mixing head geometry was evaluated using at least two separate batches of reaction solutions. One stream contained 200 mmol/L HCl and second stream contained DMP and NaOH. When determining the functional dependence of mixing time on velocity, only one mixing head, 500A-Y2X: $d = 500$ μm and $D/d = 4.76$ with a conical outlet, was used with a range of 8.6 mmol/L to 600 mmol/L HCl before mixing. Both reaction solutions contained 90 mmol/L sodium chloride and used a solvent of 25 wt. % EtOH in D.I. Water. DMP 99+% and 1.000 molar standard NaOH and HCl, were used as purchased (Aldrich). To avoid decomposition, DMP was not contacted with any material of pH less than 8 prior to a run. All solutions were formulated based on weight measurements.

The starting reaction temperature ranged from 23.0 to 26.2°C, when calculated based on the effluent temperature and the adiabatic heat rise due to reaction. This was higher, but within one degree of the average of the two reaction solution temperatures just before mixing. Therefore, a significant heat generation (due to turbulent energy dissipation) above the adiabatic temperature rise due to reaction was not detected upon mixing. Based on the mass-flow rate through the mixer, heating of the fluids due to turbulence was not expected. The maximum adiabatic temperature rise was 3.8°C, small enough to avoid a significant spatial variability in the rate constants (due to temperature segregation) to effect the reaction conversion (Baldyga et al., 1998). The characteristic reaction time reported in the results section was determined using Eqs. 23 and 3 and was based on the calculated starting temperature, the starting salt concentration, and the concentration of B if mixed instantaneously and no reaction had occurred.

Prior to each run, the pressure transducers were calibrated with nitrogen and all nitrogen was removed from the system by flushing with 25 wt. % ethanol (Aldrich 99+% or 200 proof) in D.I. water. Solutions were made as described above, charged into 100 cm^3 glass syringes and loaded onto the syringe pump(s). Although stable, starting solutions were used within 11 h. As an additional check, the starting reaction solution from each run was verified to have inconsequential decomposition before and after all samples were analyzed by gas chromatography. This indicates there is no exchange of methoxy groups with ethoxy groups during aging. All experiments used a 1:1 volume ratio for the impinging streams. The mixing system was then filled with sufficient reaction solutions to displace the 25 wt. % EtOH in water. The desired flow rate was delivered through the mixing system at constant pressure for a minimum of 4 residence times, based on the mixing chamber plus any volume before sample collection. Averaged samples of at least one-half a residence time were taken. More than one reaction sample was collected for each time the syringes were loaded by resetting the programmed flow rate to a new value and waiting for a sufficient time prior to sample collection. Samples were immediately capped after collection and placed on dry ice until GC analysis.

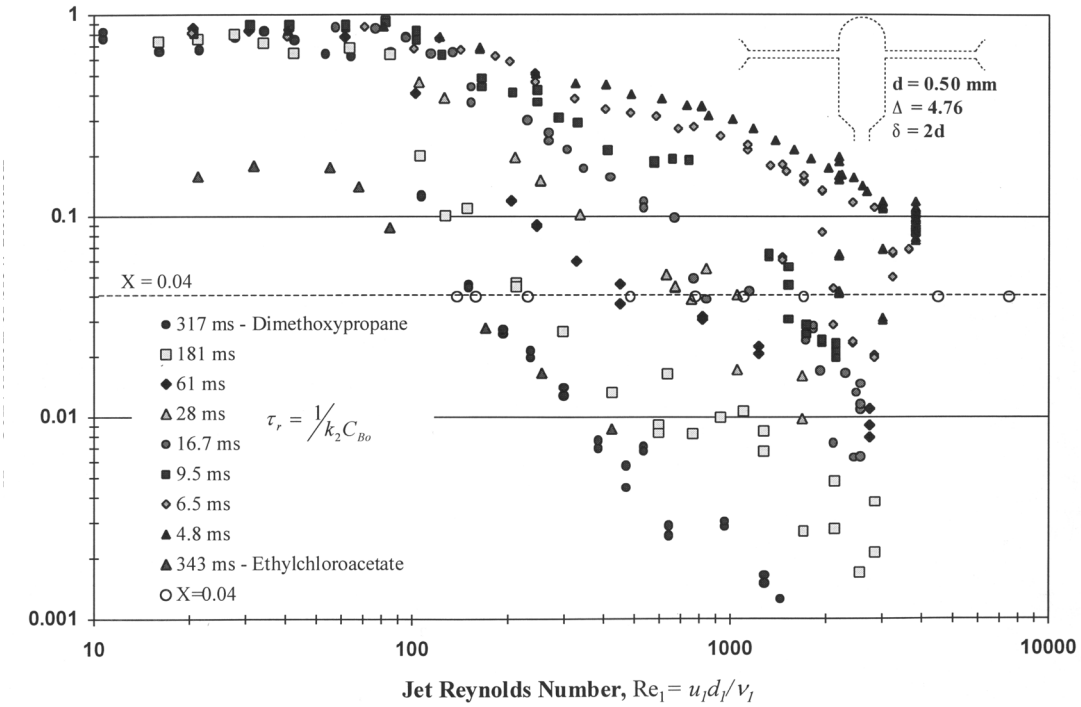

Figure 5. Competitive reactions in a CIJ Mixer at a spectrum of reaction times.

The Reynolds number was altered using the velocity of the two streams. The onset of turbulentlike flow is detected at a Reynolds number near 90. The graph displays the Reynolds number (velocity) of each data set where $X = 0.04$ for use in Figure 6.

The dimethoxypropane samples were analyzed on a Hewlett Packard 6890 gas chromatograph controlled using HP Chemstation software. The unit was equipped with a cooled sample tray held at 5°C as a precaution to limit sample decomposition, a Merlin microseal septum, a 30 m column model RTX 1701, and a flame ionization detector. The best results were obtained with a split injection at a temperature of 58°C, injection volume of 0.5 μL, and an oven temperature of 35°C held for 3 min before ramping to a higher temperature. Samples over 200 mmol/L starting concentration were diluted with pH = 12 D.I. water prior to analysis. A calibration curve was constructed each day reagent solutions were made by running the reactions in Eqs. 20 and 21. To ensure complete decomposition of the DMP, varying amounts of Stream 2, containing the DMP and NaOH, were added to a molar excess of Stream 1 containing the HCl. The generation of methanol was quantified and ethanol was used as an internal standard. As expected, the calibration curves for each day overlapped and a single curve was used for all results. The reaction conversion for a run was calculated based on the generation of methanol and the loss of DMP was monitored. The mass balance over the starting DMP closed, $100 \pm 4\%$.

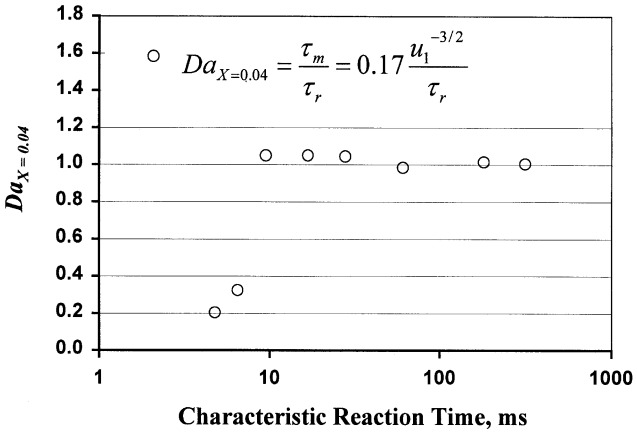

Figure 6. Damköhler number vs. characteristic reaction time for the competitive reactions of neutralization and dimethoxypropane acid hydrolysis.

The graph displays when the scaling model of Eq. 19 fails to capture the process physics. Deviation is expected to be reaction specific.

Observations

Dependence of mixing time on velocity

Figure 5 displays the fractional conversion X of many runs at different characteristic reaction times (different C_{B0}) in the 500A-Y2X mixing chamber: $d = 500$ μm, $\Delta = 4.76$, conical outlet, and $\delta = 2d$, plotted as a function of jet Reynolds number. The plot represents a Reynolds number from 10 to 3,820, a jet velocity from 0.04 to 16.0 m/s, and a residence time in the mixing chamber from 2,940 to 7.8 ms, respectively. Below a Reynolds number of 50, there is considerable scatter in the data and an improvement in mixing with the Reynolds number cannot be verified. As shown in Figure 5, there is a transition for all the runs at a Reynolds number near 90 where the conversion begins to drop. This transition is the change from a laminar behavior to a more chaotic or turbulent-like behavior as has been shown using computer simulations (Wood et al., 1991; Unger et al., 1998) and using flow visualization (Lee et al., 1980; Tucker and Suh, 1980; Sandell et al., 1985). The transition for the base hydrolysis of ethylchloroacetate is less pronounced since the minimum value of conversion begins at a lower value. Since the reaction is not catalytic and the original length scale of the fluid striations in the jet mixer is small, equal to the jet diameter or 500 μm, a conversion of only 0.2 at a Reynolds number of 10 was approached. If the fluids were perfectly segregated and a 1:1:1 mole ratio A:B:D was used, the maximum conversion of ethylchloroacetate would be $X = X_Q = 0.5$ (Bourne and Yu, 1994). Since the DMP hydrolysis is catalytic, in perfectly segregated conditions, the conversion would approach one. In the present study, the conversion approached a value over $X = 0.7$ at a Reynolds number of 10.

Above the transition to turbulent-like flow at a *Re* near 90, the mixing quality steadily improves as indicated by the decrease in DMP conversion. As discussed in the introduction, this is in contrast to many RIM studies where a limiting Reynolds number was reported to exist, often between 200 and 600, beyond which no further improvement was experienced. We attribute this finding to the sensitivity of the mixing probe to characteristic mixing times less than 350 ms. As expected, a higher Reynolds number (note that only velocity was changed for each data set) is required to obtain an equivalent conversion as the characteristic reaction time becomes faster or is reduced. Based on the scaling model presented in Eq. 18, the characteristic mixing time changes as the inverse of the velocity to the three halves power. For this article, we assume the relation between X and Da is unique. Thus, if we determine the Reynolds number (velocity) at a constant X as a function of τ_r, we can test the scaling model for τ_m with respect to velocity. These estimates of the Reynolds number are provided in Figure 5 for $X = 0.04$. In Figure 6, the ratio of the characteristic times or Damköhler number according to Eq. 19 (multiplied by an arbitrary constant to force $Da = 1$) are plotted vs. the characteristic reaction time for a conversion of $X = 0.04$. The scaling model correlates the process performance well from 340 to 9 ms, as shown by a constant Damköhler number. Thus, the mixing time in the system scales as $\tau_m \propto u^{-3/2}$. At a characteristic reaction time of 6.5 ms, it is possible one or more of the model assumptions are no longer a good physical approximation and the model does not fit the results. As shown in Figure 5, the 6.5 ms and 4.8 ms runs appear to break away from the rest of the runs, even at low Reynolds numbers. This signifies the behavior may be specific to the reaction conditions and not a change in the mixing mechanism.

The dependence of characteristic mixing time on velocity was tested by Nguyen and Suh (1985) by mixing three jets, two reactive and one inert. They found the inert domain size λ_d captured within the reacted polymer varied as $\lambda_d \propto u^{-3/4}$. Since the characteristic mixing time is proportional to the square of the characteristic length scale, as in Eq. 7, we find again the characteristic mixing time is directly proportional to $u^{-3/2}$. This relation held from a Reynolds number of 300 to 4,000.

Dependence of process performance on Damköhler number

We can examine the turbulence scaling model over all conversion values by plotting X vs. Damköhler number accord-

ing to Eq. 19. As shown in Figure 7, a direct relationship between conversion and *Da* exists for the parallel reactions, $\gamma = 1$

$$X = \beta Da^{\gamma} \tag{28}$$

The relationship holds for two orders of magnitude and covers characteristic reaction times from 340 to 9 ms. Provided the flow is turbulent, both the catalytic DMP hydrolysis and noncatalytic ethylchloroacetate hydrolysis follow Eq. 28. Therefore, this relation should hold for other parallel reactions similar to those discussed in Eq. 2. This makes a facile prediction of results within the same geometry. A single reaction condition can be examined and the reaction conversion at other reagent concentrations or other flow rates can be known *a priori*. The transition from laminar to turbulent-like flow is also clear in Figure 7. For the 317, 181, and 61 ms data sets, the conversion remains at a high value >0.7, characteristic of laminar flow. As the Reynolds number is increased or the Damköhler number is decreased, the conversion suddenly drops to the conversion characteristic of turbulence. A smaller Damköhler number is reached before the transition as the characteristic reaction time is increased.

The relationship in Eq. 28 with $\gamma \approx 1$ may also hold for competitive and consecutive reactions of Eq. 5, but only when the selectivity X_S, as defined in Eq. 6, replaces X

$$X_S \propto Da \tag{29}$$

For a single data set of Kusch et al. (1989) (Figure 8) and for a Reynolds number up to 500, the process performance as measured by selectivity to S, X_s, was directly proportional to $u^{-3/2}$. This suggests that the selectivity is proportional to Damköhler via Eq. 19 when the characteristic mixing time follows Eq. 18.

Elucidation of mixing mechanism

The characteristic mixing time based on momentum diffusion in Eq. 18 scales with kinematic viscosity to the half power. If molecular diffusion was limiting in the mixing process, the mixing time would scale with viscosity to the three halves power and, if turbulent diffusion or inertial convective mixing were active, there would be no dependence on viscosity. In order to discern which mixing process is active, 20,000 g/mol poly(ethylene oxide) (PEO) was added to each feedstream in order to change the viscosity of the combined stream by a factor of 3.6, from 2.0 to 7.1 mPa·s, while keeping the density of the streams constant. The diffusion coefficients for the reagents have been shown to vary little ($<20\%$) when an inert low molecular weight polymer is employed at low concentrations. Likewise, we do not expect the reaction kinetics to change significantly since the same reagent concentrations were used for each run. Several runs were made with and without PEO as shown in Figure 8. Additional scatter in the two sets of data is greater than the other experimental results in the article primarily due to the use of a hand injection G.C. vs. an automated G.C. used for all other experimental results.

In Figure 8, scaling the characteristic mixing time by momentum diffusion $\tau_m \propto \nu^{1/2}$ captures the data well compared to a molecular diffusion model $\tau_m \propto \nu^{3/2}$. In addition, if the mixing mechanism was turbulent diffusion or inertial convective in nature, the characteristic mixing time would scale as the inverse of velocity $\tau_m \propto u^{-1}$, not as the inverse of velocity

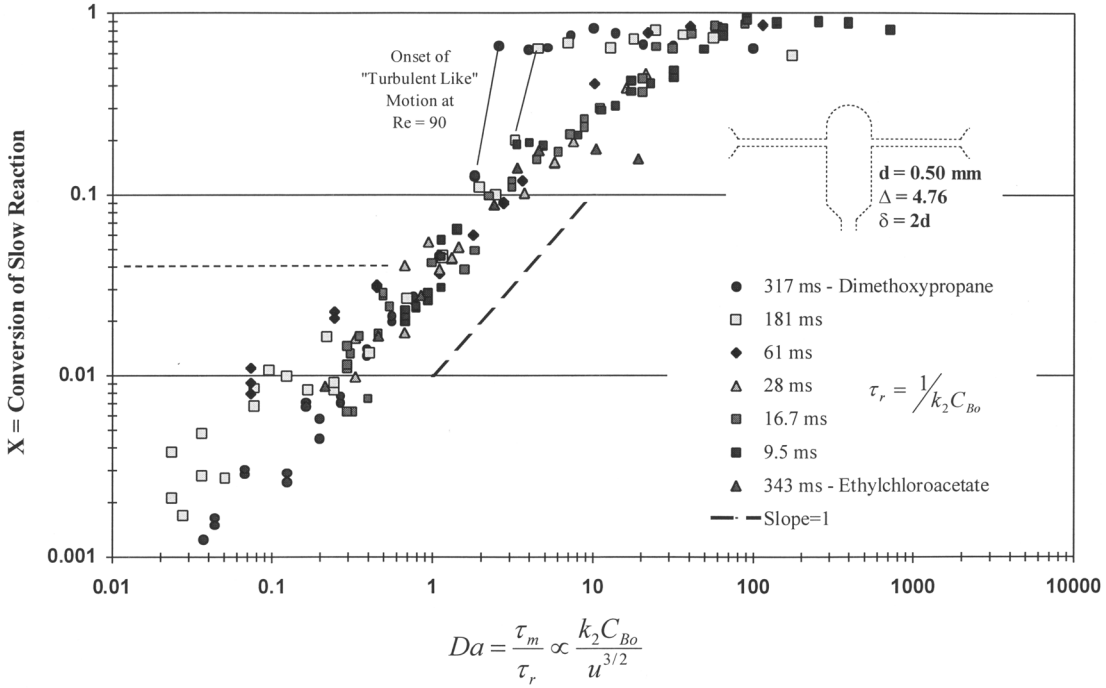

Figure 7. Conversion of slow competitive reaction versus Damköhler number.

Demonstrates $\tau_m \propto u^{-3/2}$, and the conversion of the slow reaction is directly proportional to Damköhler number for competitive reactions in the form of Eq. 2.

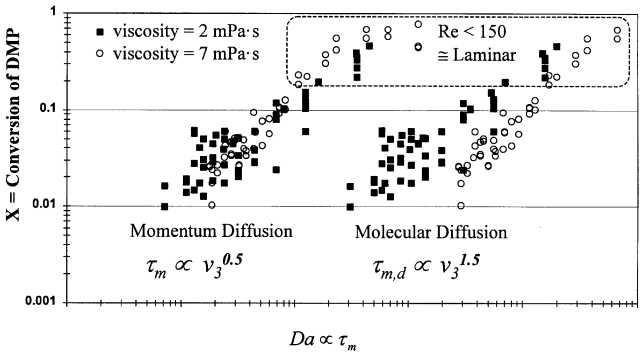

Figure 8. Elucidation of mixing mechanism by a change in system viscosity to change momentum diffusivity.

Momentum diffusion is the active mixing mechanism over molecular diffusion since the process performance scales as $\tau_m = \nu^{1/2}$ (the two data sets overlap). In this and several following figures, the *Da* is multiplied by a constant to separate the data sets used to test each scaling.

to the three halves power $\tau_m \propto u^{-3/2}$, as verified by Figures 6 and 7. Therefore, we find momentum diffusion is the active mixing mechanism and it is correct to use the momentum diffusivity not molecular diffusivity in Eq. 7.

Dependence of mixing time on geometry

To determine the scale-up behavior of confined impinging jets and the functional form and size of the mesomixing volume in Eq. 9, a number of mixing heads of different geometry were constructed, as shown in Figure 4 and Table 1. For these studies, the characteristic reaction time was held constant by using a constant reagent concentration of $C_{Bo} = 100$ mmol/L at a similar temperature.

Table 1. Dimensions and Configuration of Mixing Heads Used for Processing

Mixing Head	Jet d, mm	Chamber Multiple, Δ	Outlet Type	Outlet Multiple	Outlet δ, mm
250A-Y2X	0.25	4.76	Conical	2	0.50
250A-S4X	0.25	4.76	Square	4	1.00
250B-S4X	0.25	9.52	Square	4	1.00
250C-Y2X	0.25	19.0	Conical	2	0.50
250C-S4X	0.25	19.0	Square	4	1.00
250C-S12.7X	0.25	19.0	Square	12.7	3.18
500A-Y2X	0.50	4.76	Conical	2	1.00
500A-S2X	0.50	4.76	Square	2	1.00
500A-S6.3X	0.50	4.76	Square	6.4	3.18
500A-M6.3X	0.50	4.76	Mixer	6.4	3.18
1000A-Y2X	1.00	4.76	Conical	2	2.00

Scale-Up of the CIJ Mixer. The characteristic mixing time presented in Eq. 18 relies on the construction of a mesomixing volume of unknown geometric dependence and size. Regardless of dependence on the chamber multiple, the mesomixing volume can be expressed as proportional to the jet diameter cubed and the Damköhler number is proportional to the jet diameter to the half power, as developed for Eq. 19. Figure 9 displays the conversion vs. Damköhler number for a direct scale-up of all mixing head dimensions. Jet diameters of 250 μm, 500 μm, and 1,000 μm, and a constant chamber multiple $\Delta = 4.76$ were tested. The characteristic reaction time was 15 ms for the 1,000 μm jet diameter data set instead of 16.7 ms for the other data sets due to a slightly higher reaction temperature. This small difference is cor-

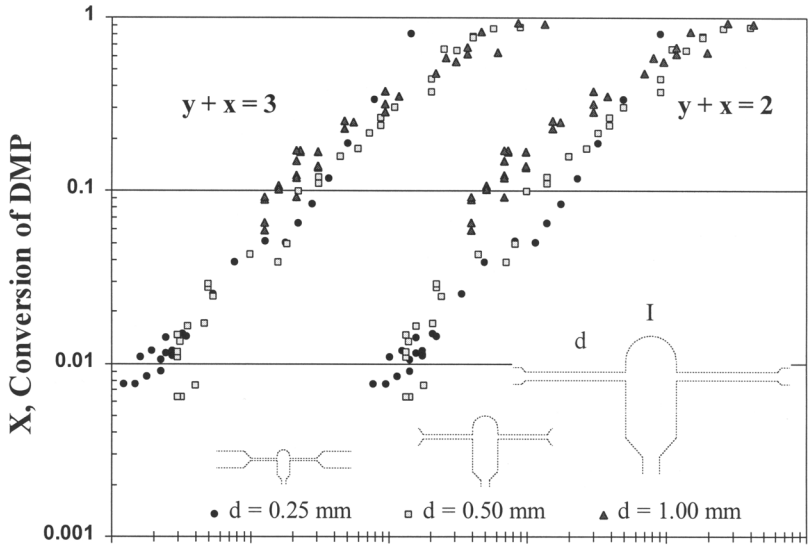

$$Da \;\alpha\; \frac{\tau_m}{\tau_r} \;\alpha\; V_m^{1/2} d^{-1} \frac{u^{-3/2}}{\tau_r} \;\alpha\; d^{(y+x-2)/2} \frac{u^{-3/2}}{\tau_r}$$

Figure 9. Scale-up of the CIJ Mixer with $\Delta = 4.76$ *d* and a conical outlet.

Verification of Eq. 18 dependence on jet diameter and the dimensional consistency ($y + x = 3$) of the mesomixing volume.

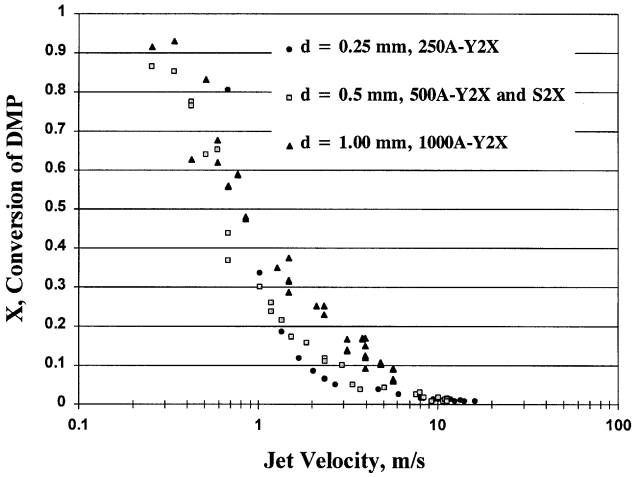

Figure 10. Scale-up of the CIJ Mixer with $\Delta = 4.76\ d$ and a conical outlet.

Demonstrates equal process performance that is not obtained when scale-up is by equal velocity. A geometric correction (Eq. 31) is required.

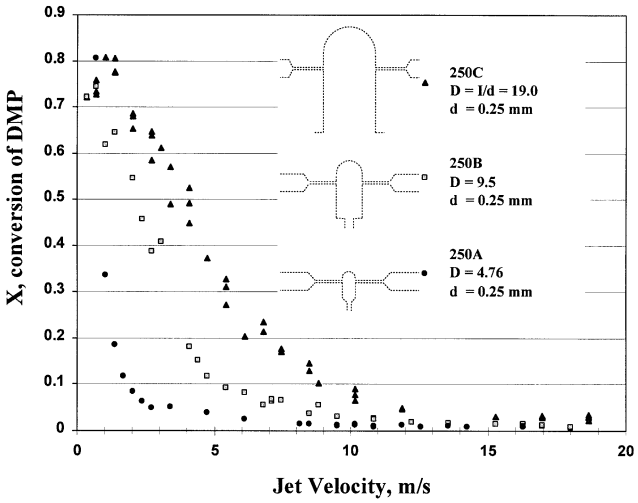

Figure 11. X vs. jet velocity as a function of chamber multiple, $\Delta = l/d$ (internozzle separation).

A large increase in jet velocity is required for the same mixing performance as the chamber size increases.

rected for by the dependence on velocity in the Damköhler number, as discussed in the previous section.

As required by Eq. 16, the data collapses onto a single curve and the best fit of the data is when $y + x = 3$ vs. $y + x = 2$. Investigators who have studied mixing by submerged free impinging jets have suggested jet velocity as the important scale-up variable (Mahajan and Kirwan, 1996; Schaer et al., 1999). Figure 10 displays the direct scale-up runs plotted vs. jet velocity, a measure of residence time. Maintaining the same velocity upon scale-up is not sufficient to ensure equivalent process performance and a small geometric correction is required. If constant velocity were assumed to scale-up processing in the impinging jets mixer, the exponent of the jet diameter in Eq. 18 would be zero. This is dimensionally unsound because the Damköhler number would have units. In turn, this implies the mesomixing volume would have dimensions of an area $y + x = 2$ in Eq. 16. Therefore, we find for the CIJ mixer, direct scale-up can be accomplished by maintaining a constant characteristic mixing time

$$\tau_{\text{mix}} \propto \frac{d^{1/2}}{u^{3/2}} \tag{30}$$

and a small correction to velocity as

$$u_{\text{new}} = u_{\text{old}} \left(\frac{d_{\text{new}}}{d_{\text{old}}} \right)^{1/3} \tag{31}$$

Dependence of the Mesomixing Volume on Internozzle Separation. The dependence of mesomixing volume on the internozzle separation or chamber diameter was examined by changing the chamber multiple from $\Delta = 4.76$ to 9.5 to 19.0 at a constant jet diameter of 250 μm. As shown in Figure 11, the effect of the chamber multiple is quite pronounced. A considerable increase in jet velocity or jet Reynolds number is required to obtain equivalent mixing performance (conversion) as the chamber size is increased. Again, if we assume a proper expression for the mesomixing volume will yield an equivalent conversion for an equivalent Damköhler number, we can alter the exponent y, corresponding to the chamber multiple and find the smallest variation in the data sets. As shown in Figure 12, the smallest overall variation in the data was experienced when the mesomixing volume was proportional to the chamber multiple cubed, $y = 3$ in Eq. 16. The correlation was better than when the mesomixing volume was taken as proportional to the internozzle separation squared, $y = 2$. For reference, the results of the 500A-Y2X runs are included.

Mesomixing Volume Vs. Reaction Volume. Figure 13 displays the combined results for all mixing heads evaluated at a similar characteristic reaction time. Again, we are assuming the mesomixing volume is proportional to the internozzle spacing or the chamber diameter to the cube power. This implies that the mesomixing volume could be on the same order as the mixing chamber itself. As shown in Figure 14, we have altered the outlet configuration of several mixing heads in order to qualitatively evaluate the size of the reaction volume, assumed to be equal to the volume required to complete the acid neutralization. With nearly a molar equivalent of base in the system, the instantaneous neutralization of sodium hydroxide by hydrochloric acid occurs in a similar time as the solvent mixing time. The mesomixing volume for energy dissipation by the impinging jets, as defined in Eq. 9, is smaller than the reaction volume since momentum diffusion of reactants must occur to complete the reaction by homogenization. Thus, we can use the reaction volume as an upper estimate of the mesomixing volume.

The undesired reaction of DMP with hydrochloric acid can only occur if the neutralization reaction and mixing process is incomplete. Therefore, if the reaction volume is the size of the entire chamber, a change in the outlet configuration can change the deformation history of the fluid and show a significant effect on the process performance, as measured by conversion. The additional fluid stretching and deformation re-

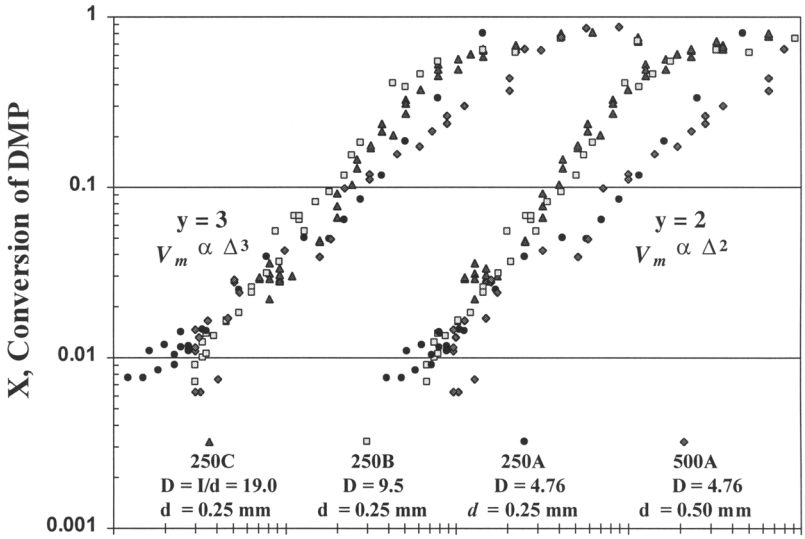

$$Da \alpha \frac{\tau_m}{\tau_r} \alpha V_m^{1/2} \frac{d^{-1}u^{-3/2}}{\tau_r} \alpha \Delta^{y/2} \frac{d^{1/2}u^{-3/2}}{\tau_r}$$

Figure 12. Determination of the functional form of the mesomixing volume.

X vs. *Da* as a function of internozzle separation. The best correlation of the data is obtained by $y = 3$ or $Da \propto \Delta^{3/2}$.

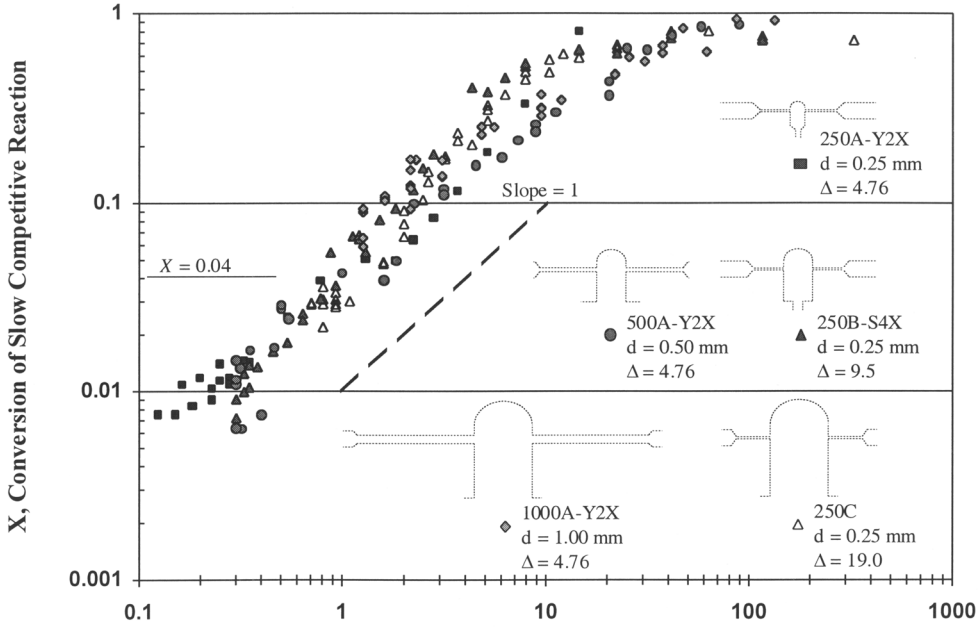

$$Da = \frac{\tau_m}{\tau_r} = K_{CIJ} \frac{1}{2\sqrt{2}} \frac{\nu^{1/2} \Delta^{3/2} d^{1/2}}{u^{3/2}} \frac{k_2 C_{Bo}}{1}$$

Figure 13. Process performance *X* vs. Damköhler number for competitive reactions of neutralization and acid hydrolysis of dimethoxypropane for each CIJ Mixer evaluated.

Demonstrates that the scaling theory for micromixing time in Eq. 19 with $y = 3$ captures the data. The constant $K_{CIJ} = 1{,}470$ when $X = 0.04$ corresponds to a Damköhler number and a flow ratio of unity.

quired to exit the mixing chamber through a tube of small diameter is significant if the reaction or mixing process is not complete. We designed our standard confined impinging jet mixer with a small outlet just for this reason to rapidly finish the mixing process if required.

In the smallest chamber $\Delta = 4.76$, the diameter of the outlet tube affected the conversion, which demonstrated that the volume of the reaction zone extended beyond the volume of the cavity for the small chamber. Although more pronounced for the 250 μm jet diameter, both the 250 μm and 500 μm jet diameter exhibited a significant increase in conversion (slower mixing) by simply increasing the diameter of the outlet tube, $\delta = 2d$ to $4d$ and $\delta = 2d$ to $6.4d$, respectively. At a Reynolds number approaching 100 and residence time approaching 250 ms, conversion is effected by the outlet diameter and the reaction volume is at least the size of the mixing chamber. These results indicate the reaction volume and possibly the mesomixing volume is on the order of the mixing chamber for a chamber multiple of $\Delta = 4.76$. The cylindrical corner formed at the bottom of the mixing chamber by changing from a cone to a square outlet did not cause enough back mixing to effect the conversion, as shown in Figure 14 for the 500 μm chamber with a $\delta = 2d$. Some investigators have recommended a static mixer following the impingement chamber can help improve process performance of a RIM style mixer. Also in Figure 14, we have tried placing an alternating helical static mixer, 1/8 in. ID (Kenics), directly after the 500 μm jet diameter with a $\Delta = 4.76$ and $\delta = 6.3d$. Any benefit was small and clearly less than simply reducing the outlet tube diameter. We would not expect a large effect on the process since the residence time in a single mixing element is larger than the chamber residence time and the scale of segregation would be reduced slowly. Likewise, the characteristic reaction time was always less than the residence time of the mixing head plus the first element of the mixer. Notice that in the case of acid base neutralization, the reaction volume changes little with characteristic reaction time since the neutralization is instantaneous. The characteristic reaction time only changes the conversion for DMP obtained within the reaction volume.

The reaction volume and mesomixing volume are less than the chamber volume when the chamber multiple is increased to $\Delta = 19.0$. For the 250 μm jet diameter, the outlet configuration had no effect on the reaction conversion and the mixing is completed prior to reaching the chamber outlet. This is the reason we have highlighted the internozzle spacing as the key scaling variable instead of the chamber diameter in Eq. 16. Based on the above results, we expect the conversion from free impinging jets, where the chamber diameter has no effect on process performance, to confined impinging jets occurs between a chamber diameter of 4.8 d to 19 d.

Transition from Confined to Free Impinging Jets. It is interesting to compare our results to those in the literature. Benet et al. (1999) studied two submerged free jets impinging at 180° in a large tank at Reynolds number from 5,000 to 20,000 (5 to 20 m/s). They directly observed the fading of a co-fed dye due to the neutralization of sodium hydroxide with a 5% excess of hydrochloric acid, the same molar ratio as our experiments, except the acid was in excess. The volume to complete the decolorization reactions was not explicitly stated, but appeared from the figure to be as much as twice the height of the radial core of the impinging jets, similar to a mesomixing volume. The height of the radial core was approximately 5.5 d, 6 d, and 8 d for internozzle spacings $\Delta = 5$ d, 10 d and 20, respectively, and changed little over the high Reynolds numbers evaluated. Our confined impinging jets had a chamber height of 3.8 d, 7.6 d, and 15.2 d and a chamber radius of 2.4 d, 4.8 d and 9.5 d, respectively. Therefore, if undisturbed by jet outflow, the radial core of an impinging jet can be contained within a chamber multiple near $D/d = 10$, and

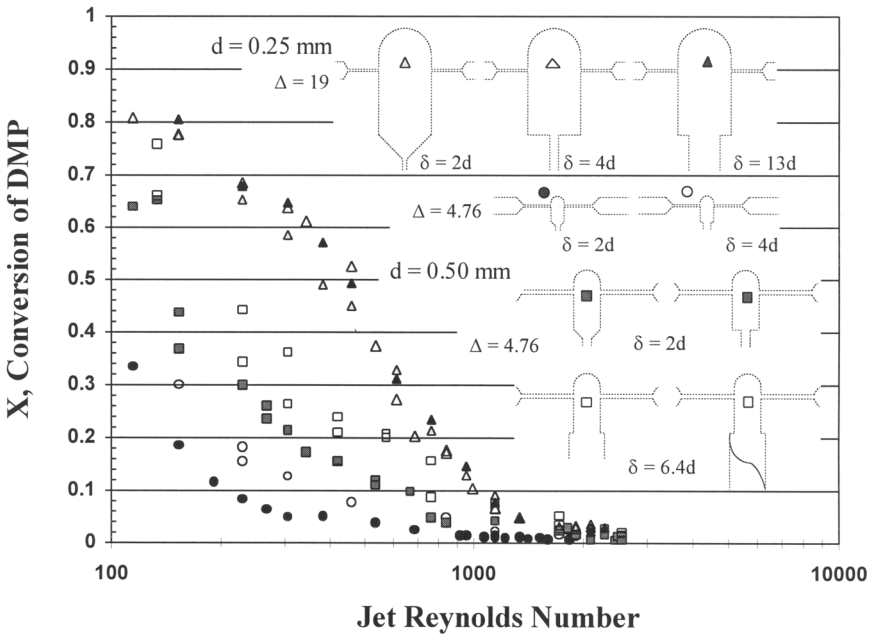

Figure 14. Determination of reaction volume via observing the effect of the mixer outlet.

X vs. *Re* where only velocity was changed.

the reaction volume for acid base neutralization can be contained in a chamber multiple of $D/d = 20$. Therefore, the transition from confined to free impinging jets occurs between a D/d of 10 to 20.

Processing in Confined Impinging Jets

The functional relationship of micromixing time to Reynolds number and chamber geometry has been debated in the past. The results of the relevant studies are summarized in Table 2. It is clear the characteristic mixing time is proportional to the inverse of the velocity to the three halves power. All previous studies reported this functionality for the Reynolds number by changing velocity. Tucker and Suh (1978) were the first investigators to suggest this relationship to Reynolds number, but their experimental data was not precise enough to prove it. The results of Lee et al. (1980) were taken at low Reynolds numbers, data points between 100 and 200, and could have been convoluted by the transition from laminar behavior to turbulent-like behavior occurring near a *Re* of 90 to 150.

The dependence of characteristic mixing length on Reynolds number was determined by Nguyen and Suh (1985) by measuring the domain size λ_d of an inert phase captured within the polymerization of the two other jet streams. In Table 2 we assume the chacteristic mixing time is proportional to the square of the characteristic length scale. Again, regardless of three impinging jet streams and possible effects of interfacial tension, their results agree well with our findings using single-phase chemical reactions. Unfortunately, they did not disclose the details of their mixer and offered no relationship for the dependence of mixing time on system geometry.

Kusch et al. (1989) did not address the topic of mixing time directly, but we were also able to extract the functional relationship of characteristic mixing time from their work. The selectivity to S, X_s as in Eq. 6, was found to be directly proportional to the inverse of the Reynolds number to the three halves power. Therefore, via the process scaling theory including Eqs. 19 and 29, we assume the characteristic mixing time has the same dependence on Reynolds number. They also only investigated a single mixing head, so the effect of the mixer geometry could not be determined.

Mahajan and Kirwan (1996) were the first to quantify the mesomixing volume for twin impinging jets, but their development was incomplete. They failed to provide a third dimension for the mixing volume. They rationalized the unknown dimension as possibly a fraction of the internozzle separation, but also stated earlier in the article that the internozzle separation had no effect. We have not resolved this question since we have not changed the internozzle spacing independently from the chamber diameter. As with all the other previous investigations, a molecular diffusion mechanism instead of momentum diffusion was assumed and the effect of viscosity was not tested.

The dependence of characteristic mixing time for confined impinging jets on velocity appears well founded by previous research, but the dependence on geometry is system specific. The mesomixing volume, or the region of high mixing intensity, as defined in the process scaling theory of this article, is a construct to help envision and model the mixing process. The actual energy dissipation is not uniform and varies throughout the mesomixing volume, as shown by the CFD simulation of Schaer et al. (1999). Likewise, all the kinetic energy of the jet streams are assumed to be used to determine the initial length scale for momentum diffusion. Thus, no energy would be available for futher momentum diffusion below the Kolmogorov length scale. Our results simply indicate that the best approximation for homogeneous processing in confined impinging jets is found by taking this mesomixing volume as proportional to the internozzle spacing cubed to yield Eq. 32

$$\tau_m = K_{CIJ} \frac{\nu_3^{1/2} \Delta^{3/2} d_1^{1/2}}{u_1^{3/2}} \frac{1}{2\left(\frac{\rho_1}{\rho_3}\right)^{1/2}\left(1+\frac{m_1}{m_2}\right)^{1/2}} \qquad (32)$$

It is interesting to note that one cannot discern between a momentum diffusion or molecular diffusion mechanism without changing the diffusivity, since both resulting models have the same dependence on velocity (energy dissipation rate). By changing the system viscosity at a constant diffusion coefficient, we have shown momentum diffusion to be the active mechanism for the CIJ mixer here (Figure 8). The important implication of the momentum diffusion mechanism is that the mixing process has little dependence on the diffusion coefficient of the reagents in the system. The maximum dependence on $Sc = \nu/D_{AB}$ is $\tau_m \propto$ arcsinh $(0.05Sc)$ (Baldyga and Pohorecki, 1995; Johnson, 2003). Therefore, when applying Eq. 32 to other chemical systems, it is not necessary to accurately measure the molecular diffusion coefficient of the reactants to determine the characteristic mixing time. The use of Eq. 32 is also limited to the range of Reynolds numbers where momentum diffusion is the active mixing mechanism, in this case from a *Re* of near 150 to a *Re* of at least 3,000 for low viscosity fluids and *Sc* near 1,000. It is important to realize there is a crossover point where inertial convective mixing becomes the active mixing mechanism (slower mixing time). This is evident in the scaling of the characteristic times

Table 2. Dependence of Micromixing Time on Velocity, Viscosity, and Chamber Geometry

	Range Evaluated			Process Output	$\tau_m \propto \frac{\Delta^A d^B \nu^C}{u^D}$				
	τ_r, ms	D/d	*Re*		*D*	*A*	*B*	*C*	Comments
Current Study	5 to 340	4.8 to 19	100–3,000	X	1.5	1.5	0.5	1	I = D
Mahajan and Kirwan (1996)	65,200	12 to 50	500–2,500	Xs	1.5	0	0		I/d = 10
Kusch et al. (1989)	$(3 \text{ to } 12)\times10^3$	5	50–500	Xs	1.5				
Nguyen and Suh (1985)	$(30 \text{ to } 180)\times10^3$	RIM	300–4,000	λ_d^2	1.5		0.5		3 Jets
Lee et al. (1980)	$(6 \text{ to } 49)\times10^3$	1.6 to 6.4	100–200	heat rise	1	−3	1		

with velocity u^{-1} for inertial convective vs. $u^{-3/2}$ for momentum diffusion, as in Figure 1. The specific mixers evaluated to generate Eq. 32 have an exit kinetic energy near one-quarter of the inlet and changes in outlet size have not been included; only direct scale-up and changes in chamber multiple were quantified in the expression. Likewise, changing the flow ratio of the two streams has not been considered here and Eq. 32 cannot be readily extrapolated to flow ratios far from 1:1. This has been addressed in separate studies on a vortex mixer (Johnson, 2003).

Absolute mixing time

Equation 32 represents the scaling relationship that we desired at the beginning of the article (Steps 1 to 5 of the Research Method), but we have yet to define the absolute mixing time via identification of the reactor constant K_{CIJ}. We can define the constant based on an estimate of the reaction volume size taken as the time to neutralize acid and base by mixing to a characteristic amount, such as 63%. Since the acid base reaction is several orders of magnitude faster than the mixing process, the mixing process is rate limiting and the time to neutralize the acid and base equals the "mixing lifetime" for the entire *process* of mixing two fluid streams. Since the DMP reaction can occur only if the acid base reaction is incomplete, observing the effect of outlet configuration of the mixer can be used to identify whether the mixing process is complete within the residence time of the mixer.

As demonstrated in the previous sections, the effect of the outlet is minimal at a $D/d = 10$ and the mixing lifetime characteristic of the process is less than the residence time at $D/d = 10$. At a $D/d = 5$, the outlet configuration has a significant effect at low Reynolds number and a limited effect at a higher Reynolds number. The point where the effect diminishes is near a Reynolds number of 2,200 for $d = 500$ μm. We conclude that the mixing is not complete in the residence time of the mixer at low velocity, but occurs on the same time-scale as the residence time at high velocity. We can identify the reactor constant by taking the mixer residence time and the mixing time to be equal at $Re \cong 2{,}200$ and solving Eq. 32. The result is that $K_{CIJ} = 1{,}470$. This value is approximate, but a different choice of Re (velocity), where the mixing time and the residence time are equal, only changes K_{CIJ} by a whole number and doesn't affect the conclusions of the article or the methodology to obtain the mixing time.

With the expression for the absolute mixing time in the CIJ mixer, we can further define a standard set of conditions for the dimethoxypropane reaction set to yield $Da = 1$. Figure 13 demonstrates graphically that $X = 0.04$ at $Da = 1$ for a flow ratio $F = 1$. Figure 6 also clearly demonstrates the result since $\tau_m = 0.17 u_1^{-3/2}$ by Eq. 32 with $K_{CIJ} = 1{,}470$ and SI units. This standard condition, $X = 0.04$ Da at $F = 1$, for the DMP reaction set can be used to find an absolute mixing time or a reactor constant for other confined mixers.

Figure 15 displays the characteristic times that have the same scaling as momentum diffusion, $\propto (\nu/\epsilon)^{1/2}$. Baldyga and Bourne (1989) have shown, with simulations for diazo couplings in a semi-batch reactor, that under conditions of $Sc <$ 4,000 and a flow ratio away from one, "engulfment" of new fluid is the rate limiting step in micromixing $\tau_{m,E} = 17.31$ $(\nu/\epsilon)^{1/2}$, not molecular diffusion. This conceptual framework

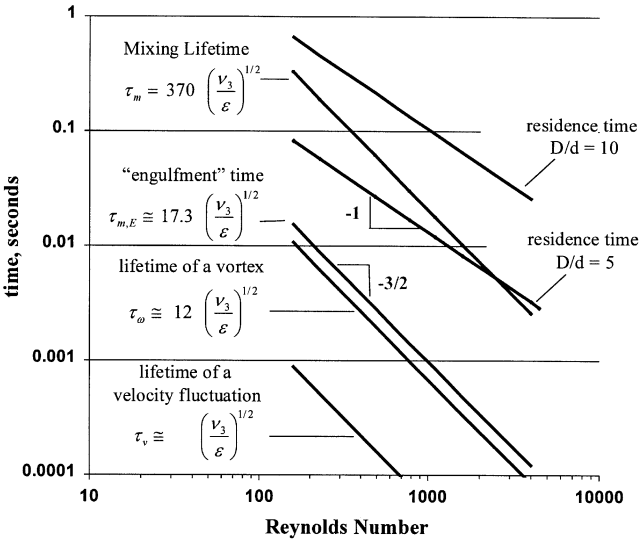

Figure 15. Times with the scaling of momentum diffusion vs. the residence time in the mixer.

The mixing lifetime is that characteristic of the entire process of mixing or many "engulfments." The value $K_{CIJ} =$ 1,470 in Eq. 32, originating from Eq. 10, was estimated by "flow visualization" studies where the effect of the outlet on reaction conversion as a function of the reactor size and flow conditions was monitored for the DMP reaction set. Details are provided in the text. This measurement provides a standard condition of $X = 0.04$ for $Da = 1$ and $F = 1$ to characterize other mixers in the future.

has the same dependence on energy dissipation rate and momentum diffusivity as the momentum diffusion model employed here. Tracing our development backward to Eq. 10 and including the constant $K_{CIJ} = 1{,}470$, the results is $\tau_m = 21.1\tau_{m,E}$. We have defined τ_m based on a *processing* output of molecularly mixed solutions. The engulfment model has been derived based on the hydrodynamic lifetime of a single vortex, $\tau_\omega = 12(\nu/\epsilon)^{1/2}$, with a correction for the incorporation rate of new fluid $\tau_{m,E} = \tau_\omega/\ln(2)$ (continuous equal volume engulfments). It does not represent the processing time, but the characteristic engulfment time for use in a set of model equations (Baldyga and Bourne, 1989). A ratio of 21.1 implies that the processing time is greater than one vortex generation or the characteristic engulfment time, as we expect. Likewise, the value of $\tau_\nu = (\nu/\epsilon)^{1/2}$ is the characteristic lifetime of a velocity fluctuation (Baldyga and Bourne, 1999), which is 12 times less than that of the vortex lifetime. With $K_{CIJ} = 1{,}470$, competitive reactions in the CIJ mixer can be represented by

$$X = 0.04Da = 0.04\frac{\tau_m}{\tau_r} = 0.84\frac{\tau_{m,E}}{\tau_r} \tag{34}$$

Here, τ_m follows Eq. 32 and τ_r follows Eq. 3.

Conclusion

An easily constructed laboratory-to-intermediate scale confined impinging jets mixing system was built and characterized to deliver rapid micromixing of two fluids. An advantage of this system is that tests can be run at the small scale with limited amounts of fluid and the process performance can be

easily duplicated at the production scale. A methodology to determine an absolute mixing time in the confined mixer was developed and followed. Using a single highly sensitive, flexible, and robust parallel reaction, the dependence of the characteristic micromixing time on the velocity, viscosity, and chamber dimensions was elucidated at both low and high Reynolds numbers and compared to previous research. The onset of turbulent-like flow in the mixing chamber was determined to occur at a Reynolds number near 90. The mixing quality, as judged by reaction conversion, was then found to improve as the velocity was increased. Micromixing times well below 9.5 ms (defined by the point where only 4% of the undesired slow reaction occurred) were easily attained.

A simple scaling theory, based on momentum diffusion from the Kolmogorov length scale, was adopted for the CIJ mixer in order to correlate the characteristic micromixing time. The single time constant model assumed that the macromixing, mesomixing, and molecular diffusion portion of micromixing are not important to determine the mixing time. The energy dissipation rate for a determination of the initial Kolmogorov length scale was taken as proportional to the kinetic energy of the impinging streams dissipated over a mass with a mesomixing volume.

Experiments verified the characteristic mixing time scaled as the inverse of the jet velocity to the three halves power, the momentum diffusivity to the one-half power, and the mesomixing volume (over which the bulk of the energy was dissipated) was best approximated as proportional to the internozzle separation cubed. Maintaining equivalent velocity on the scale-up of confined impinging jets was insufficient to achieve a constant mixing quality and a geometric correction was required (Eq. 31). In the turbulent regime, the parallel conversion (Eqs. 2 and 4) was found directly proportional to the Damköhler number over two orders of magnitude and this behavior was confirmed by examining a second parallel reaction. It was also implied that the conversion of consecutive and competitive reactions (Eqs. 5 and 6) was directly proportional to the Damköhler number. At velocities above the laminar to turbulent transition, the reaction volume for acid base neutralizations was contained within a chamber of a diameter 19 times the jet diameter, indicating submerged and free impinging jets are obtained below this size.

The characteristic mixing time and scale-up rules for turbulent confined impinging jets, including the velocity, viscosity, and geometric dependencies, is presented in Eq. 32 where the measured value of $K_{CIJ} = 1{,}470$ provides a standard condition of $X = 0.04$ for $Da = 1$ and $F = 1$ for the DMP reaction set. This is the key result of this article.

Acknowledgments

The authors would like to thank Jared Jensen for collecting the data at 5 wt. % PEO, Jersey Baldyga and John Bourne for helpful discussions, and the following for generous support of our endeavors: Merck & Co. Inc. for support of Brian under the Merck Doctoral Fellowship, Procter & Gamble Unversity Exploratory Research Program, and Rhodia Complex Fluid Laboratories.

Notation

A, B = reagents in reaction, A, B, D, Q, R, S
C_{Bo} = concentration reagent B if all streams are mixed without reaction, mol/m^3
C_i = concentration of species i, mol/m^3
C_{init} = concentration of DMP or HCl before mixing, mol/m^3
C_S = concentration NaCl after mixing process, mol/m^3
d = jet diameter, m
D = mixing chamber diameter, m
D_{AB} = molecular diffusivity, m^2/s
D_t = turbulent diffusivity, m^2/s
Da = Damköhler number, ratio of mixing and reaction time
I = internozzle separation, m
k_i = rate constant (second order) for reaction i, m^3/mol·s
K_{CIJ} = reactor constant defined by Eq. 32, unitless
K = length of exit tube runner, m
F = ratio of jet flow rates fed to the reactor
m_i = mass-flow rate of stream i, kg/s
N_i = molar flow rate of species i
P = power used for turbulent mixing, W
$Q_{F,i}$ = volumetric flow rate of stream i, m^3/s
r = specific reaction rate, mol/m^3·s
Re = Reynolds number (based on jet diameter of acid stream, d_1)
$s(t)$ = Striation thickness as a function of time, m
Sc = Schmidt number, ratio of momentum to molecular diffusivity
T = temperature, K
u_i = average velocity of stream i, m/s
V_m = mesomixing volume, m^3
V_R = mixer volume, m^3
X = conversion (D) of slow parallel reaction
X_Q = fraction of limiting reagent (B) used for slow parallel reaction
X_s = selectivity as in Eq. 6
x, y = exponents to be determined for mesomixing volume

Greek letters

Δ = dimensionless internozzle separation, I/d_1
δ = outlet diameter, m
ϵ = turbulent energy dissipation per unit mass, W/kg
η_i = viscosity of stream i, Pa·s
λ_d = segregation length scale or domain size, m
λ_k = Kolmogorov length scale, m
ν_i = momentum diffusivity or kinematic viscosity of stream i, m^2/s
ρ_i = density stream i, kg/m^3
τ_m = characteristic mixing time, mixing lifetime, s
$\tau_{m,t}$ = characteristic time for turbulent diffusion, s
τ_s = characteristic time for inertial convective mixing, s
$\tau_{m,E}$ = characteristic engulfment time, s
τ_r = characteristic reaction time, s
τ_ω = lifetime of a vortex, s
τ_ν = lifetime of a velocity fluctuation, s

Literature Cited

Baldyga, J., "A Closure-Model for Homogeneous Chemical-Reactions," *Chem. Eng. Sci.*, **49**, 1985 (1994).
Baldyga, J., and J. R. Bourne, "Distribution of Striation Thickness from Impingement Mixers in Reaction Injection-Molding," *Polymer Eng. Sci.*, **23**, 556 (1983).
Baldyga, J., and J. R. Bourne, "A Fluid Mechanical Approach to Turbulent Mixing and Chemical Reaction—Part II Micromixing in the Light of Turbulence Theory," *Chem. Eng. Commun.*, **28**, 243 (1984).
Baldyga, J., and J. R. Bourne, "Simplification of Micromixing Calculations. 1. Derivation and Application of New Model," *Chem. Eng. J. and Biochem. Eng. J.*, **42**, 83 (1989).
Baldyga, J., and J. R. Bourne, "The Effect of Micromixing on Parallel Reactions," *Chem. Eng. Sci.*, **45**, 907 (1990).
Baldyga, J., and J. R. Bourne, *Turbulent Mixing and Chemical Reactions*, Wiley, New York (1999).
Baldyga, J., J. R. Bourne, B. Dubuis, A. W. Etchells, R. V. Gholap, and B. Zimmermann, "Jet Reactor Scale-up for Mixing-Controlled Reactions," *Chem. Eng. Res. Des.*, **73**, 497 (1995).
Baldyga, J., J. R. Bourne, and B. Walker, "Non-Isothermal Micromixing in Turbulent Liquids: Theory and Experiment," *Can. J. Chem. Eng.*, **76**, 641 (1998).

Baldyga, J., and M. Henczka, "Closure Problem for Parallel Chemical-Reactions," *Chem. Eng. J. and the Biochem. Eng. J.*, **58**, 161 (1995).
Baldyga, J., and W. Orciuch, "Closure Problem for Precipitation," *Chem. Eng. Res. Des.*, **75**, 160 (1997).
Baldyga, J., and R. Pohorecki, "Turbulent Micromixing in Chemical Reactors—a Review," *Chem. Eng. J.*, **58**, 183 (1995).
Benet, N., L. Falk, H. Muhr, and E. Plasari, "Experimental Study of a Two-Impinging-Jet Mixing Device for Application in Precipitation Processes," *Industrial Crystallization*, pp. 1–10 (1999).
Bourne, J. R., "Some Reflections on My Zurich Years," *Chimia*, **50**, 239 (1996).
Bourne, J. R., O. M. Kut, and J. Lenzner, "An Improved Reaction System to Investigate Micromixing in High-Intensity Mixers," *Ind. Eng. Chemistry Res.*, **31**, 949 (1992a).
Bourne, J. R., O. M. Kut, J. Lenzner, and H. Maire, "Kinetics of the Diazo Coupling between 1-Naphthol and Diazotized Sulfanilic Acid," *Ind. Eng. Chemistry Res.*, **29**, 1761 (1990).
Bourne, J. R., J. Lenzner, and S. Petrozzi, "Micromixing in Static Mixers—an Experimental—Study," *Ind. Eng. Chemistry Res.*, **31**, 1216 (1992b).
Bourne, J. R., and M. Studer, "Fast Reactions in Rotor-Stator Mixers of Different Size," *Chem. Eng. and Processing*, **31**, 285 (1992).
Bourne, J. R., and S. Y. Yu, "Investigation of Micromixing in Stirred-Tank Reactors Using Parallel Reactions," *Ind. Eng. Chemistry Res.*, **33**, 41 (1994).
Demyanovich, R. J., "Production of Commercial Dyes Via Impingement-Sheet Mixing. 1. Testing of a Device Suitable for Industrial Applicaiton," *Chem. Eng. Proc.*, **29**, 173 (1991).
Demyanovich, R. J., and J. R. Bourne, "Rapid Micromixing by the Impingement of Thin Liquid Sheets. 1. A Photographic Study of the Flow Pattern," *Ind. Eng. Chemistry Res.*, **28**, 825 (1989).
Demyanovich, R. J., and J. R. Bourne, "Rapid Micromixing by the Impingement of Thin Liquid Sheets. 2. Mixing Study," *Ind. Eng. Chemistry Res.*, **28**, 830 (1989).
Garside, J., and N. S. Tavare, "Mixing, Reaction and Precipitation—Limits of Micromixing in an MSMPR Crystallizer," *Chem. Eng. Sci.*, **40**, 1485 (1985).
Johnson, B. K., "Flash Nanoprecipitation of Organic Actives Via Confined Micromixing and Block Copolymer Stabilization—Volume II," PhD Thesis, Princeton University (2003).
Johnson, D. A., and P. E. Wood, "Self-Sustained Oscillations in Opposed Impinging Jets in an Enclosure," *Can. J. of Chem. Eng.*, **78**, 867 (2000).
Johnson, D. A., P. E. Wood, and A. N. Hrymak, "The Effect of Geometrical Parameters on the Flow Field of an Opposed Jet Rim Mix Head: Equal Flow and Matched Fluids," *Can. J. of Chem. Eng.*, **74**, 40 (1996).
Kolodziej, P., C. W. Macosko, and W. E. Ranz, "The Influence of Impingement Mixing on Striation Thickness Distribution and Properties in Fast Polyurethane Polymerization," *Polymer Eng. Sci.*, **22**, 388 (1982).
Kusch, H. A., J. M. Ottino, and D. M. Shannon, "Analysis of Impingement Mixing-Reaction Data—Use of a Lamellar Model to Generate Fluid Mixing Information," *Ind. Eng. Chemistry Res.*, **28**, 302 (1989).
Lee, L. J., J. M. Ottino, W. E. Ranz, and C. W. Macosko, "Impingement Mixing in Reaction Injection-Molding," *Polymer Eng. and Sci.*, **20**, 868 (1980).
Macosko, C. W., *RIM: Fundamentals of Reaction Injection Molding*, Hanser, New York (1989).
Mahajan, A. J., and D. J. Kirwan, "Nucleation and Growth-Kinetics of Biochemicals Measured at High Supersaturations," *J. of Crystal Growth*, **144**, 281 (1994).
Mahajan, A. J., and D. J. Kirwan, "Micromixing Effects in a Two-Impinging-Jets Precipitator," *AIChE J.*, **42**, 1801 (1996).
Malguarnera, S. C., and N. P. Suh, "Liquid Injection Molding I. An Investigation of Impingement Mixing," *Polymer Eng. Sci.*, **17**, 111 (1977).
Marcant, B., and R. David, "Experimental-Evidence for and Prediction of Micromixing Effects in Precipitation," *AIChE J.*, **37**, 1698 (1991).
Midler, M., E. L. Paul, E. F. Whittington, M. Futran, P. D. Liu, J. Hsu, and S. H. Pan, "Crystallization Method to Improve Crystal Structure and Size," U.S. Patent No. 5,314,506 (1994).
Nguyen, L. T., and N. P. Suh, "Effect of High Reynolds Number on the Degree of Mixing in RIM Processing," *Polymer Process Eng.*, **3**, 37 (1985).
Ottino, J. M., "Description of Mixing with Diffusion and Reaction in Terms of the Concept of Material-Surfaces," *J. of Fluid Mechanics*, **114**, 83 (1985).
Paul, E. L., H. Mahadevan, J. Foster, M. Kennedy, and M. Midler, "The Effect of Mixing on Scaleup of a Parallel Reaction System," *Chem. Eng. Sci.*, **47**, 2837 (1992).
Paul, E. L., and R. E. Treybal, "Mixing and Product Distribution for a Liquid-Phase, Second-Order, Competitive-Consecutive Reaction," *AIChE J.*, **17**, 718 (1991).
Pohorecki, R., and J. Baldyga, "The Use of a New Model of Micromixing for Determination of Crystal Size in Precipitation," *Chem. Eng. Sci.*, **38**, 79 (1983).
Sandell, D. J., C. W. Macosko, and W. E. Ranz, "Visualization Technique for Studying Impingement Mixing at Representative Reynolds Numbers," *Polymer Process Eng.*, **3**, 57 (1985).
Schaer, E., P. Guichardon, L. Falk, and E. Plasari, "Determination of Local Energy Dissipation Rates in Impinging Jets by a Chemical Reaction Method," *Chem. Eng. J.*, **72**, 125 (1999).
Tamir, A., *Impinging-Stream Reactors Fundamentals and Applications*, Elsevier Science, Amsterdam (1994).
Tucker, C. L., and N. P. Suh, "Impingement Mixing—a Fluid Mechanical Approach," *Soc. of Plastic Engineers 36th Ann. Tech. Conf.*, Washington, DC (1978).
Tucker, C. L., and N. P. Suh, "Mixing for Reaction Injection-Molding. 1. Impingement Mixing of Liquids," *Polymer Eng. Sci.*, **20**, 875 (1980).
Unger, D. R., and F. J. Muzzio, "Laser-Induced Fluorescence Technique for the Quantification of Mixing in Impinging Jets," *AIChE J.*, **45**, 2477 (1999).
Unger, D. R., and F. J. Muzzio, and R. S. Brodkey, "Experimental and Numerical Characterization of Viscous Flow and Mixing in an Impinging Jet Contactor," *Canad. J. of Chem. Eng.*, **76**, 546 (1998).
Wood, P., A. Hrymak, R. Yeo, D. A. Johnson, and A. Tyagi, "Experimental and Computational Studies of the Fluid Mechanics in an Opposed Jet Mixing Head," *Phys. Fluids A*, **3**, 1362 (1991).
Yeo, R. W., "A Numerical Study of Jet-to-Jet Impingement in a Mixing Head," PhD Thesis, Dept. of Chemical Engineering, McMaster University Hamilton (1993).
Zhao, Y., and R. S. Brodkey, "Averaged and Time-Resolved, Full-Field (Three-Dimensional), Measurements of Unsteady Opposed Jets," *Can. J. of Chem. Eng.*, **76**, 536 (1998).

Manuscript received Mar. 25, 2002, revision received Feb. 23, 2003, and final revision received Apr. 21, 2003.